University of Brighton

Kazan Federal UNIVERSITY

Advanced Engineering Centre, University of Brighton

Research Seminar

Thursday, 13th October 2016

Aerosols: environmental, technological and health science applications

S.K. Zaripov

Kazan Federal University, Kazan, Russia

Definition

Aerosol is a suspension of solid or liquid particles in a gas.

Examples: dust, clouds

Bioaerosols: aerosols of biological nature (viruses, bacteria, fungi, spores, pollens)

Aerosol sources

Nature aerosols

clouds

Smoke from forest fires Sheremetyevo 2010 08 07

industrial fire

Sea aerosols

Dust-storm-Texas-1935

car emissions

tobacco smoke

sneeze = 100,000 particles
traveling at 200 mph

sneeze particles

Aerosol particle sizes

The range of diameters of aerosol particles is **10^{-8} -10^{-4} m=0.01-100 μm=10 - 10^{5} nm**. The lower limit of **0.01 μm =10nm** roughly corresponds to the transition from molecule to particle. Particles larger than **100μm** normally do not remain suspended in air for a sufficient amount of time.

Particle terminology

Ultrafine particles or nanoparticles **r<0.2 μm**

Fine particles: **r<1 μm**

Coarse particles: **r>1 μm**

Respirable suspended particulate matter (RSP): **r<10 μm**

$PM_{2.5}$: particulate matter of size **r<2.5 μm**, **PM_{10}**: **r<10 μm**)

The mechanical and optical behaviors of particles are significantly affected by size of the mean free path for air λ~0.07 μm and the wavelength of the visible light: λ~0.4-0.7 μm.

Shape of typical aerosol particles
J. of Aerosol Science

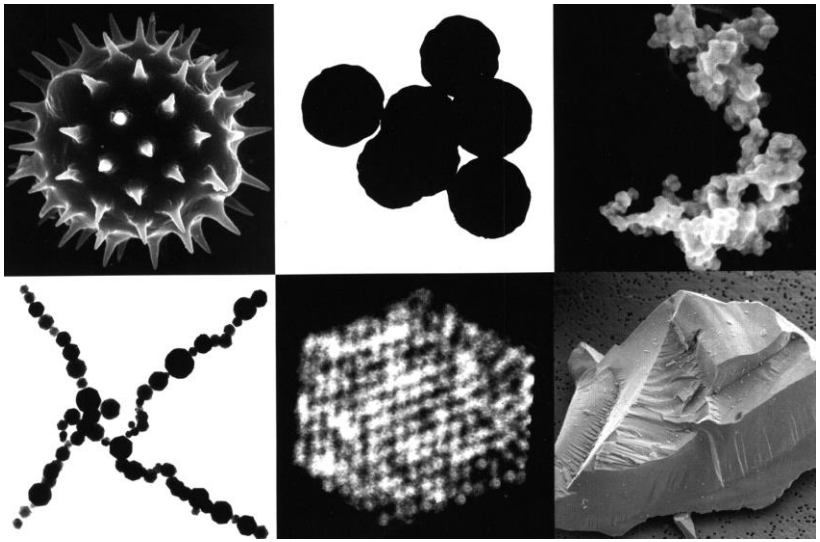

Aerosol problems

Monitoring
Health related problems
Air cleaning – air flitration
Aerosol technology

Course aerosols
Inertia
Gravity
Ultrafine particles
Diffusion
Phoretic forces (thermophoresis, diffusiophoresis, photophoreis)
Electrostatic forces

Terminology: particle size fractions

Human inhalability - aerosol influence

Environment	Workplace	
	inhalable	< 100 µm
PM10	thoracic	
	respirable	< 10 µm
PM2.5		
PM1		< 5 µm
PM0.1	Ultrafine	
Nanoparticles	Nanoparticles	

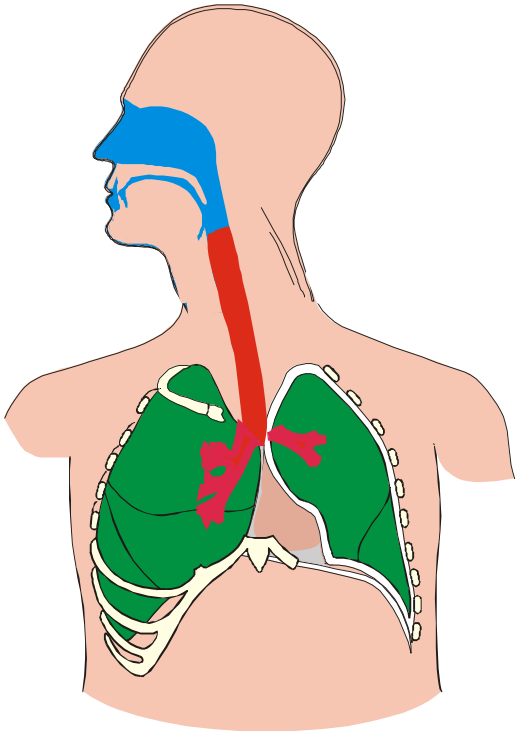

From the lecture of Prof. W.Koch, Fraunhover ITEM, June, 2014, Kazan

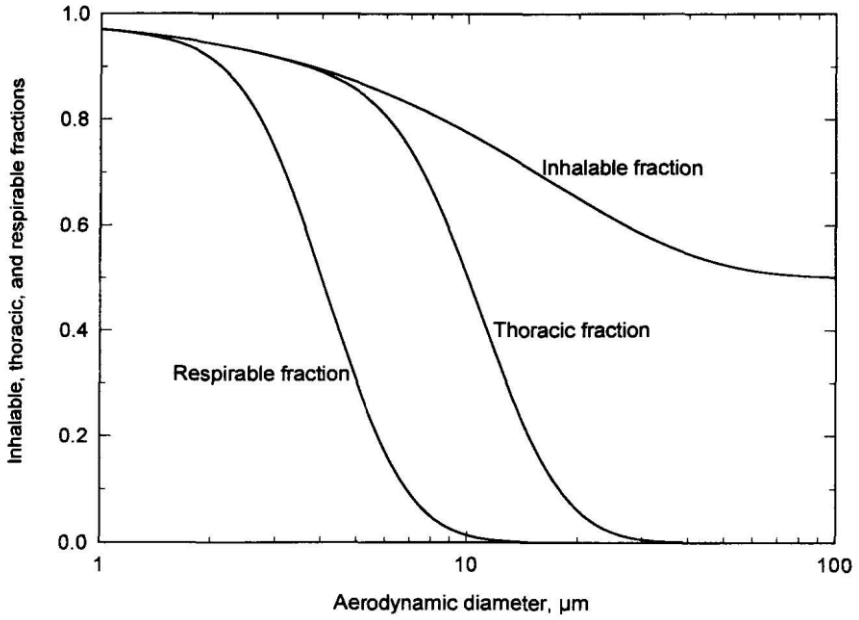

Curves of inhalable, thoracic and respirable dust fractions

Aerosol monitoring – aerosol sampling
Various sampler inlets

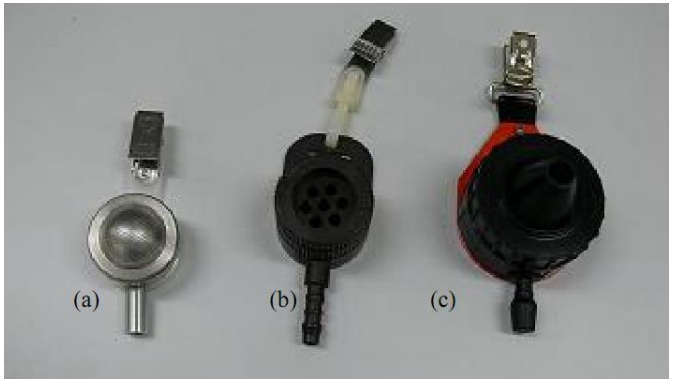

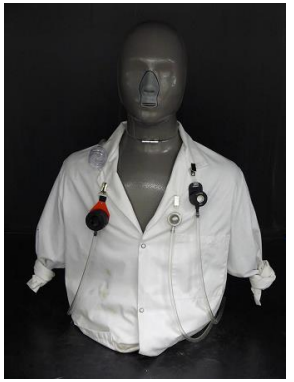

Darrah K. Schmees , Yi-Hsuan Wu and James H. Vincent

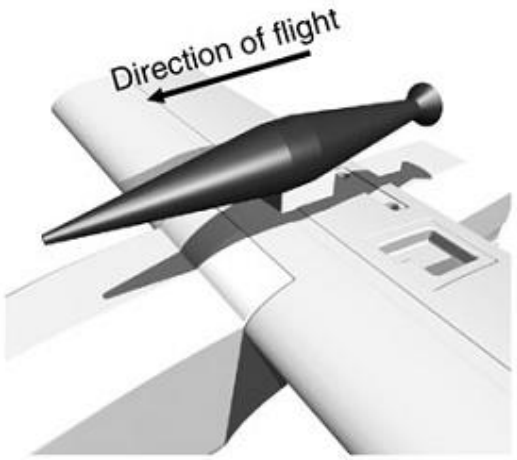

Respicon

K. Peräjärvi[1,*], J. Lehtinen[2], R. Pöllänen[1] and H. Toivonen[1]

Aspiration efficiency

$$A = \frac{c_i}{c_0}$$

c_i **concentration inside the sampler**

c_0 **concentration far from the sampler**

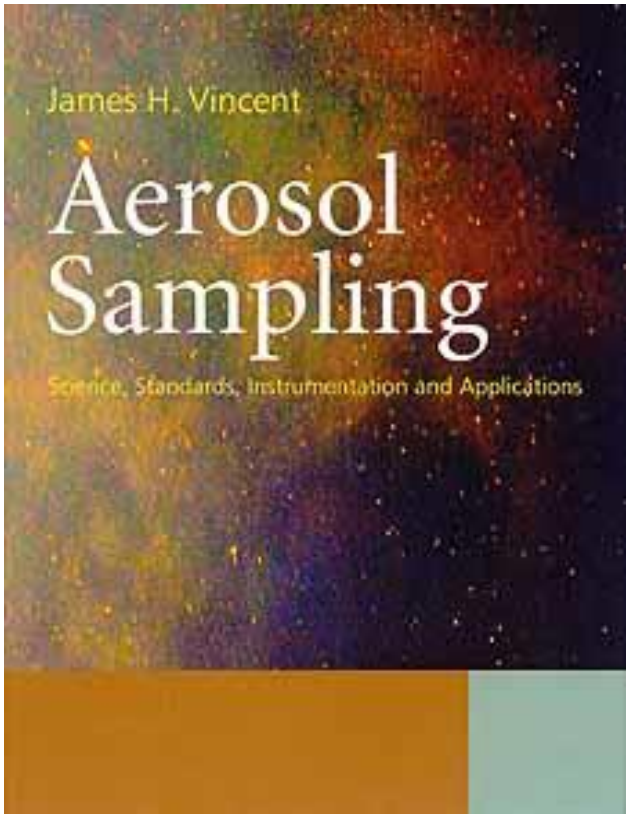

$$A = f(R_a, d_p, \rho_p, L_i, \mathrm{St}, v_s, \mathrm{Re}, B)$$

Sampling in moving air

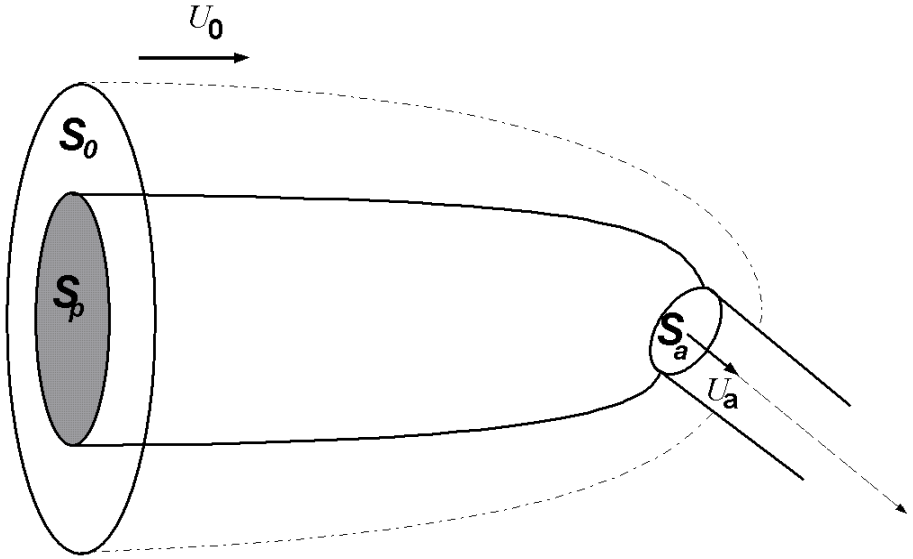

$$A(t) = \frac{N_a(t+\Delta t)}{N_0(t)} = \frac{\int_{S_a} c_a(x,y,t+\langle\Delta t\rangle) v_{pa}(x,y,t+\langle\Delta t\rangle) dydx}{\int_{S_0} c_0(x,y,t) v_{p0}(x,y,t) dydx}$$

$$A(t) = \frac{\int_{S_p} c_p(x,y,t) v_{pp}(x,y,t) dydx}{\int_{S_0} c_0(x,y,t) v_{p0}(x,y,t) dydx}$$

$$A = \frac{S_p}{S_0}$$

Lagrangian equations of particle motion

$$m\frac{d\bar{v}}{dt} = m\beta\left(\bar{u}-\bar{v}\right) + m\bar{A}\left(t\right) + m\bar{g} + \bar{F}_e$$

Aerodynamic drag — **Brownian force** — **gravity force** — **electrostatic force**

$\beta = 3\pi\,\mu\,d\,/\,c_s\,m$

$\bar{v} = \bar{v}(x,y,z)$ **particle velocity**

$\bar{u} = \bar{u}(x,y,z)$ **air velocity**

μ **viscosity**

d **particle diameter**

m **particle mass**

c_s **Cunningham correction factor**

Thin walled sampler for very small velocities ratio $R_a = \frac{U_0}{U_a}$

S.K. ZARIPOV, A.K. Gilfanov, D.V. Maklakov Numerical study of thin-walled sampler performance for aerosols in low windspeed environments. **Aerosol Science and Technology, 2010.**

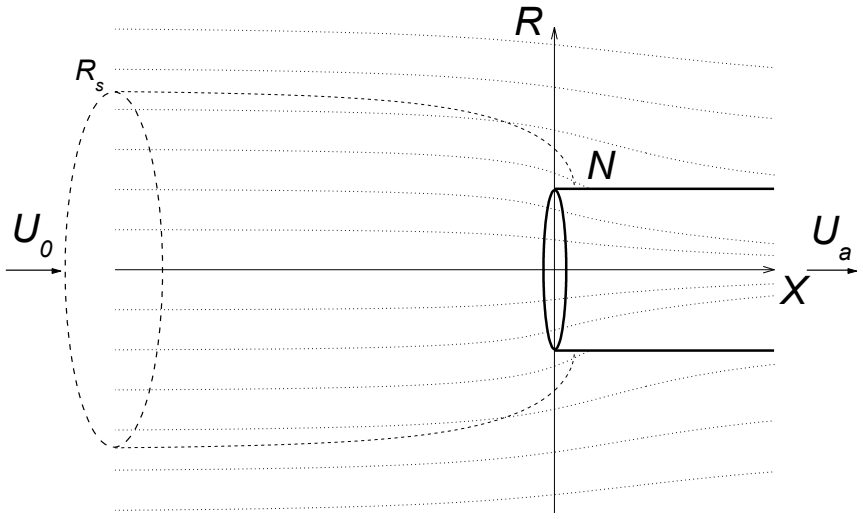

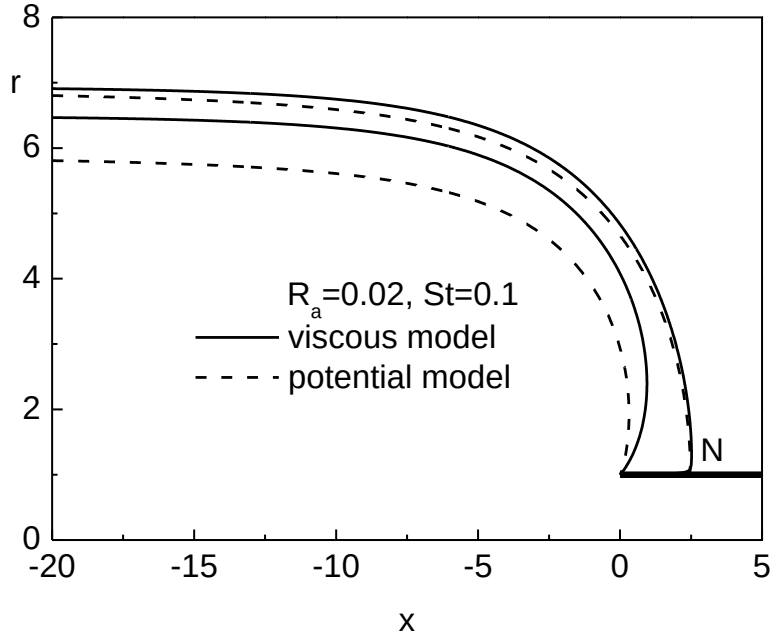

Comparison of Ai(Ra) и Ae(Ra) and experimental data Gibson&Ogden (1977) и Davies&Subari (1982)

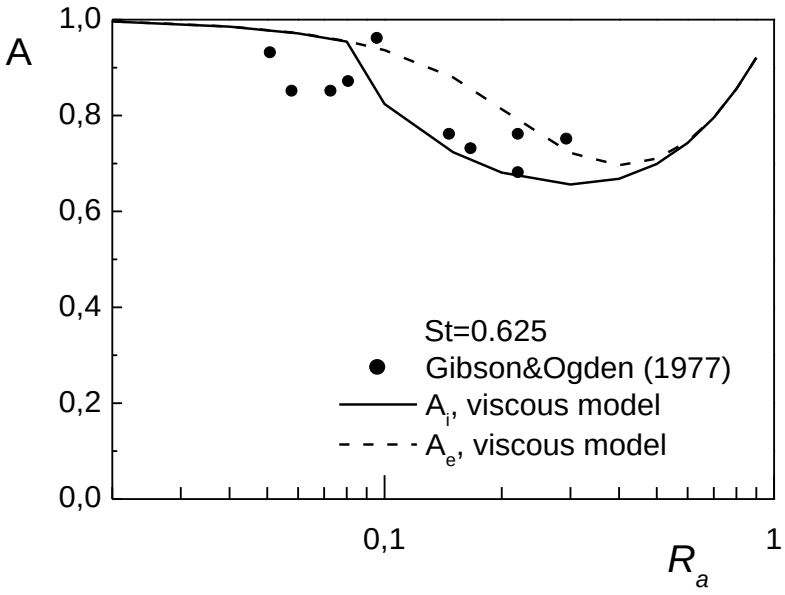

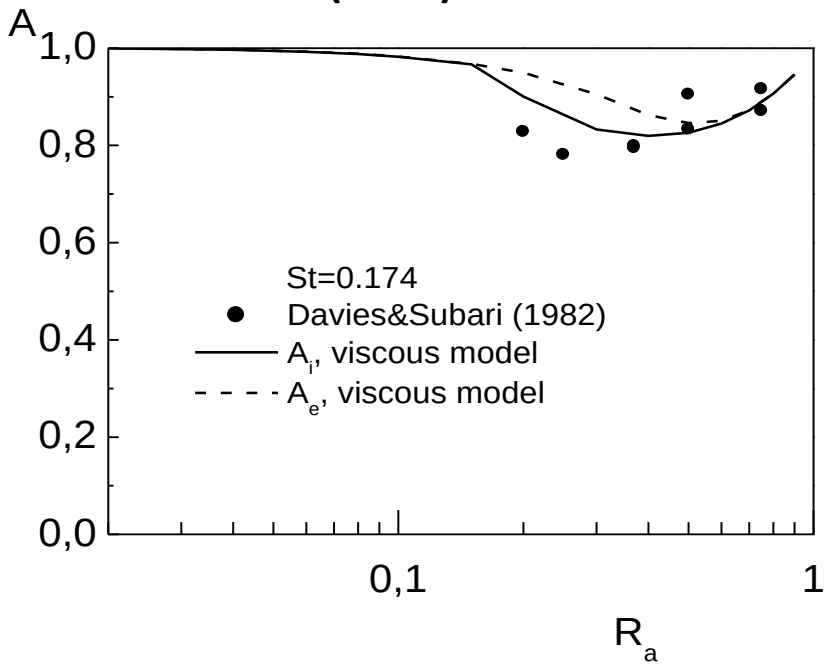

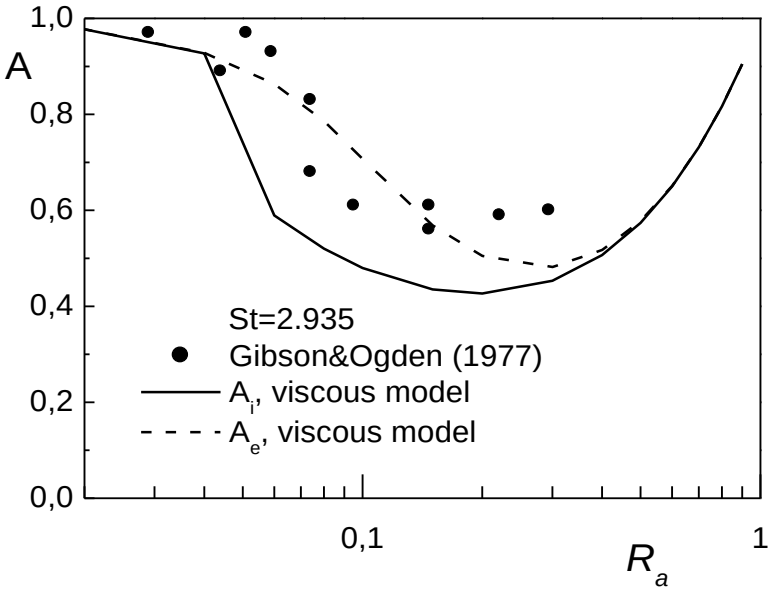

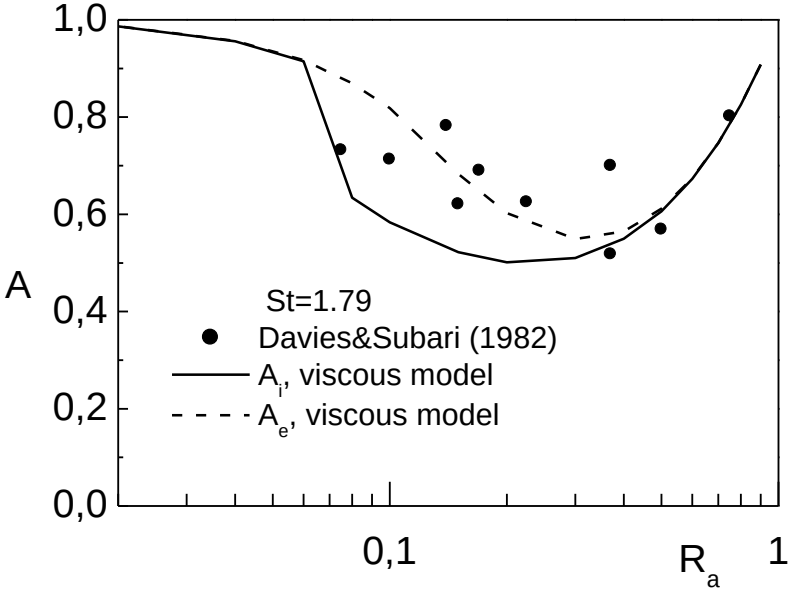

Gravity force influence

The sampled particles areas for small *Ra at* St=1.

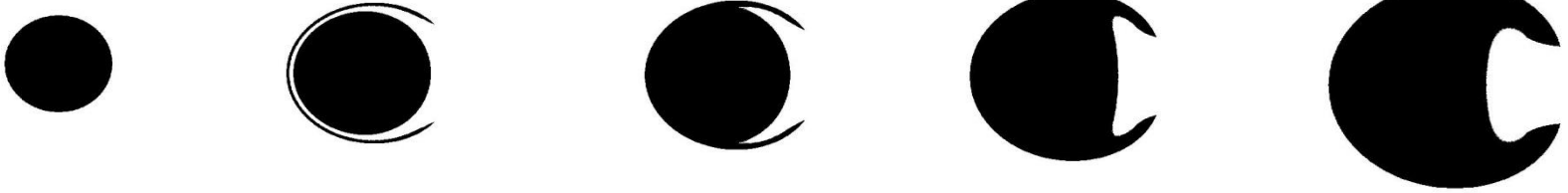

R_a=0.2 R_a=0.1 R_a=0.08 R_a=0.04 R_a=0.

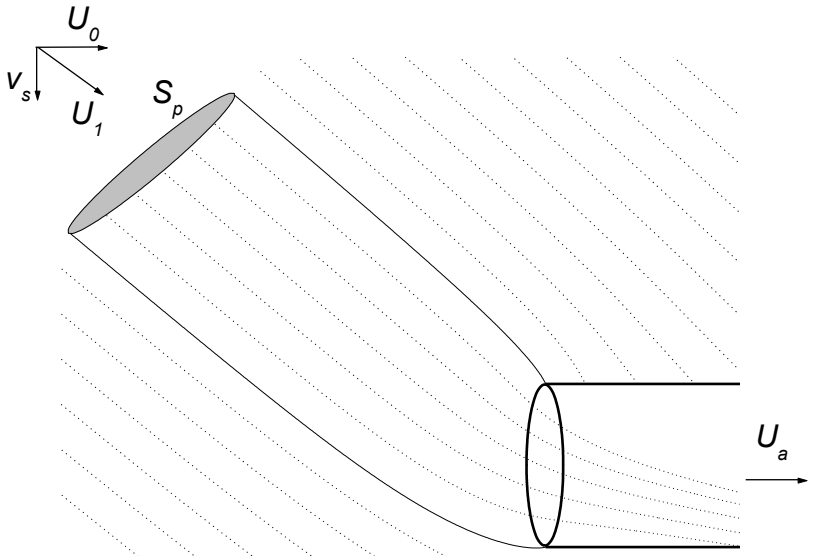

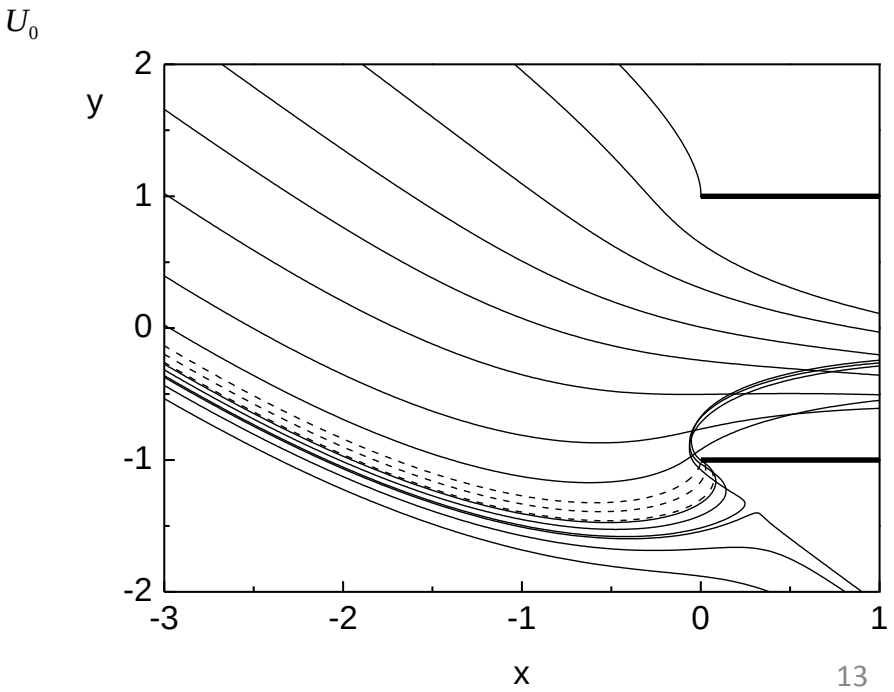

Particle concentration contours for a=0.2 (lines – particle trajectories)

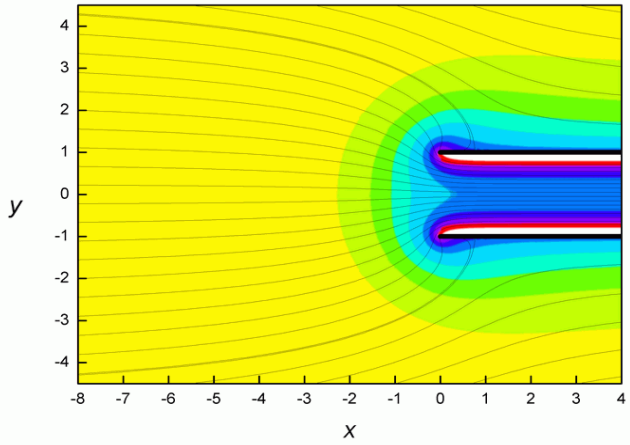

St=0.01

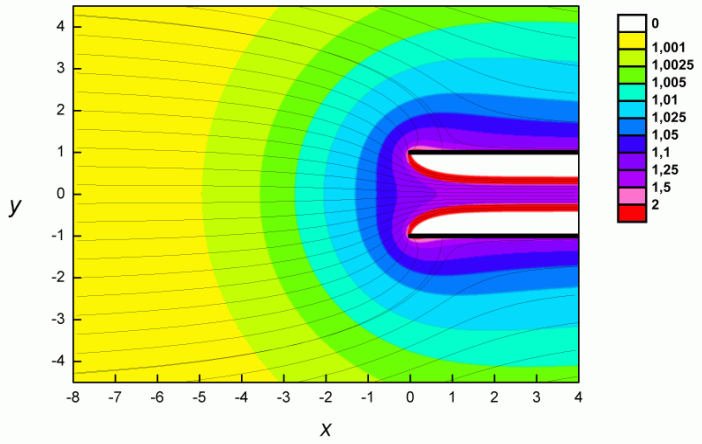

St=0.1

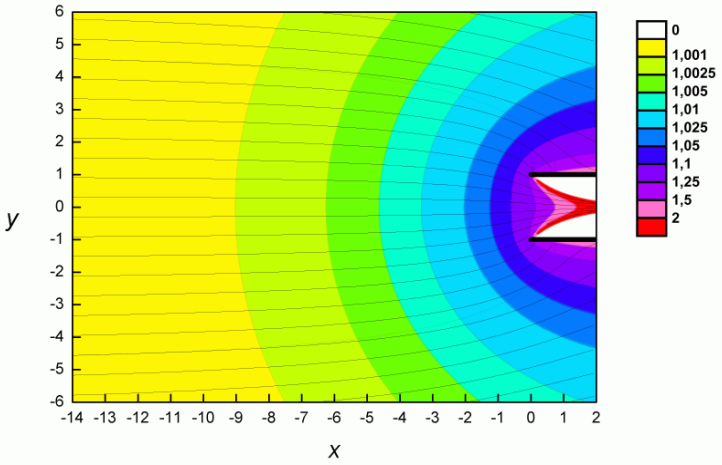

St=1

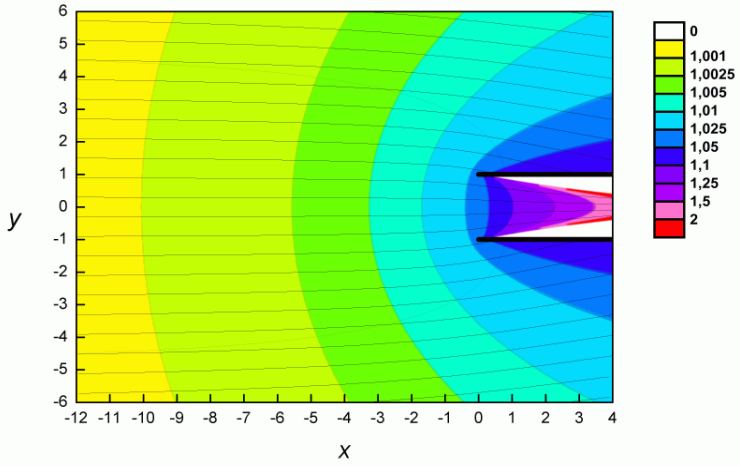

St=10

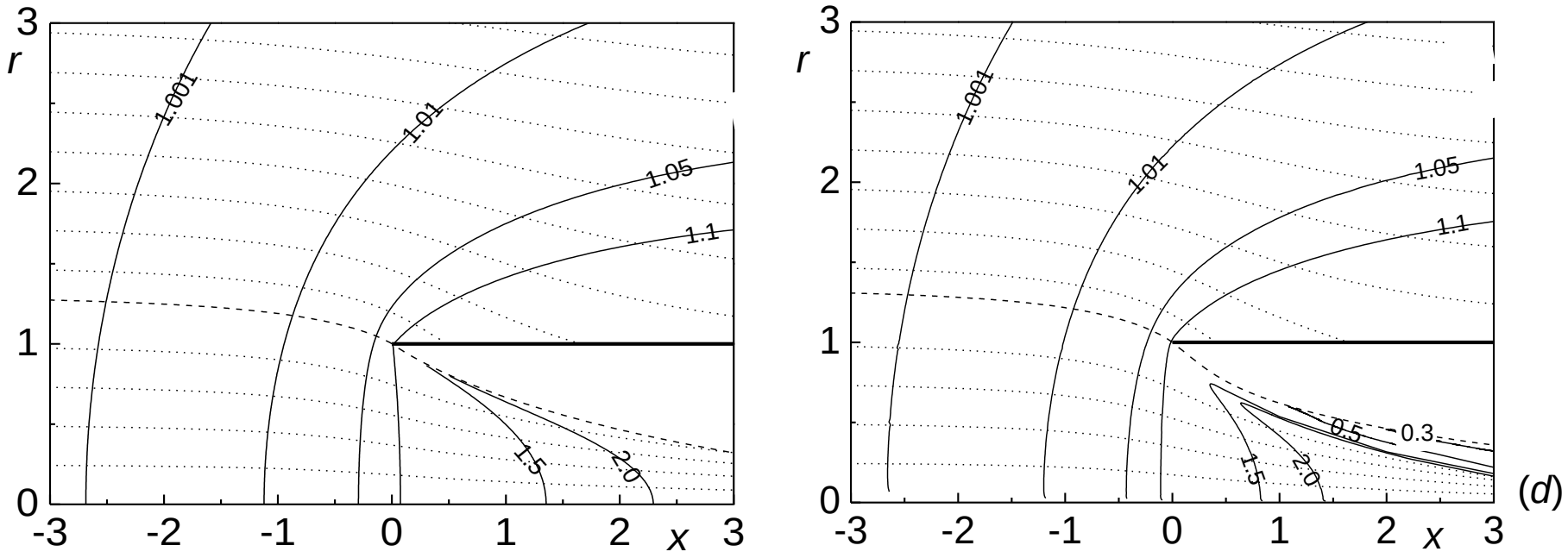

Particle trajectories and concentration isolines
R_a=0.2 and St= 1 for potential and viscous flows

Numerical study of performance of the RespiCon sampler in calm air

Zaripov S.K., Koch W. , Aerosol Science and technology, 48:74-80, 2014

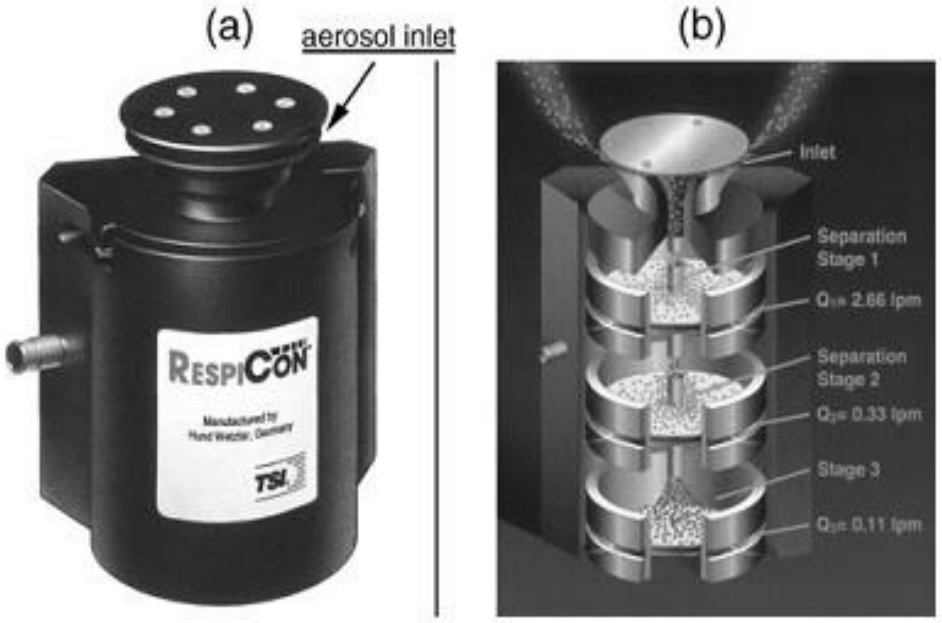

Fig. 1. Picture and schematic drawing of the RespiCon sampler. Source: catalog of TSI, Inc.

W. Koch et.al., 2009

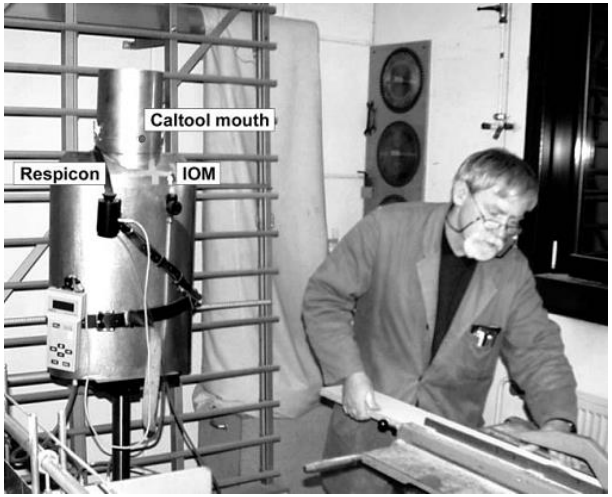

FRAUNHOFER INSTITUTE TOXIKOLOGIE UND EXPERIMENTELLE MEDIZIN, HANNOVER

Numerical study of performance of the RespiCon sampler in calm air

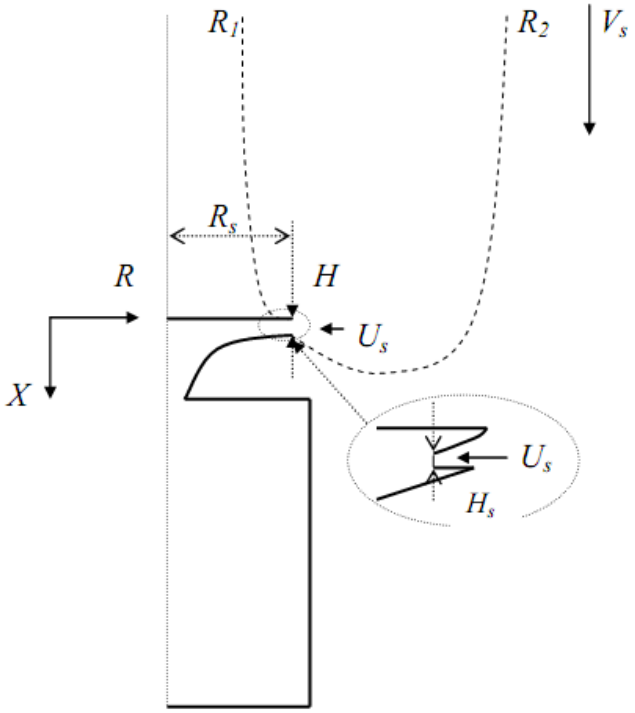

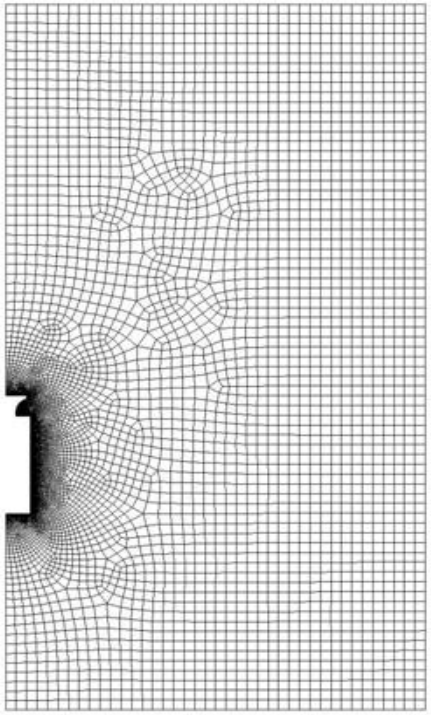

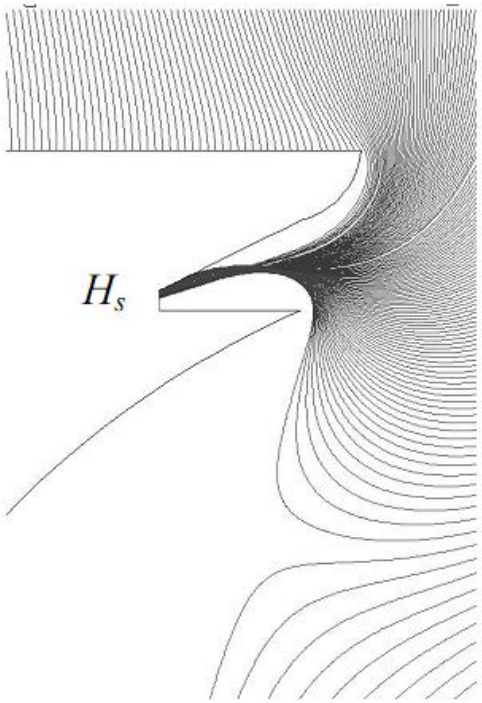

Fig. 2. RespiCon sampler scheme and mesh of calculation domain outside the sampler.

Fig. 4. Example of trajectories of particles impacting the slit wall

Collection efficiencies of RespiCon stages as a function of particle diameter

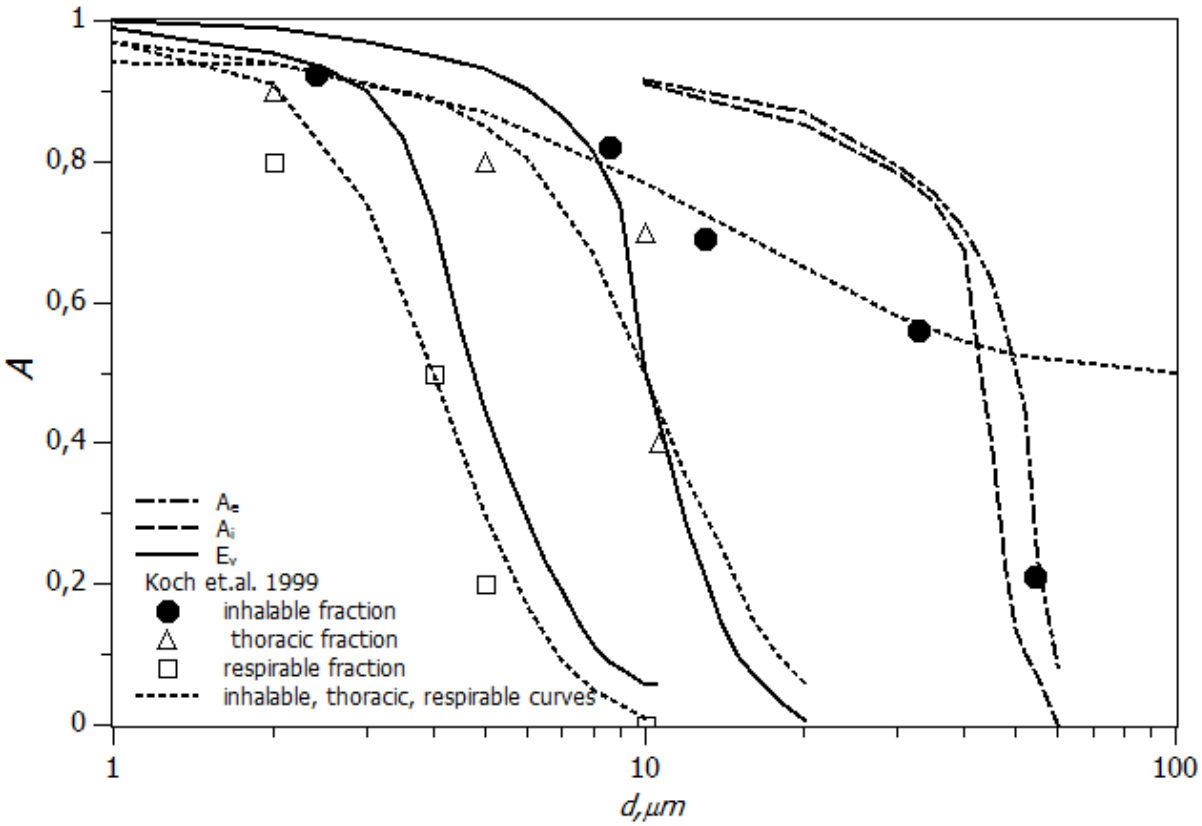

Sampling into a spherical sampler from low wind velocity environment

Galeev, R.S., and Zaripov, S.K. (2003). A theoretical study of aerosol sampling by an idealized spherical sampler in calm air. ***J. Aerosol Sci***. 34: 1135–1150.

Zaripov, S.K., Gilfanov, A.K., and Mukhametzanov, I.T. (2014). Performance of spherical aerosol sampler in low–velocity agriculture environment. ***Acta Hort.*** *(ISHS)*, 1054: 333–339.

The spherical geometry of a sampler was chosen as the particle behavior around it is similar to that around a breathing human head.

$\bar{U}_0$ **wind velocity**

$\bar{U}_s$ **sampling velocity**

$\bar{V}_s = \tau \bar{g}$ **settling velocity**

$\tau = \rho_p d_p^2 / 18\mu$

aspiration efficiency

$$A = \frac{U_1 S_p}{Q} = \frac{S_p \sqrt{U_0^2 + V_s^2}}{S_m U_s}$$

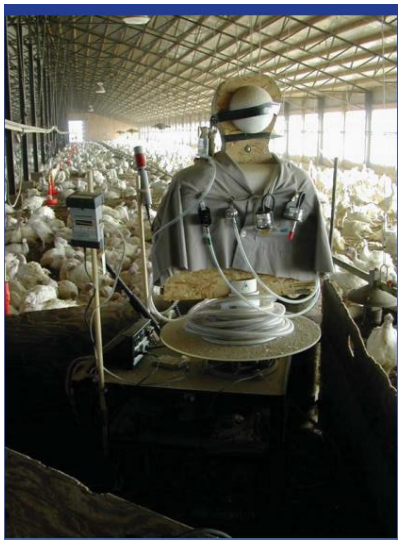

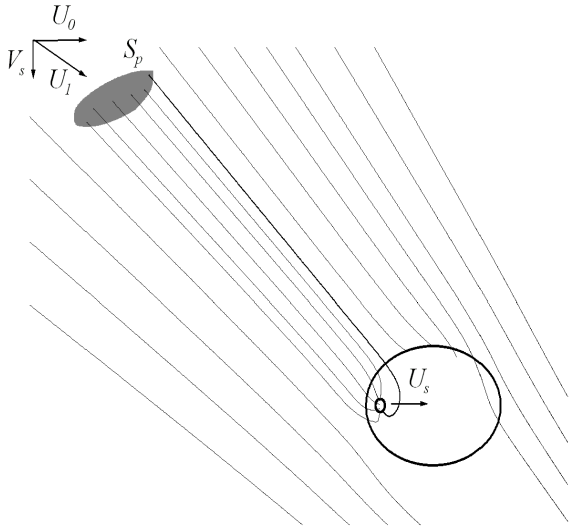

$$\bar{U}_1 = \bar{U}_0 + \bar{V}_s$$

Sampling into spherical sampler in calm air

$\bar{U}_0 = 0$ R_a=0

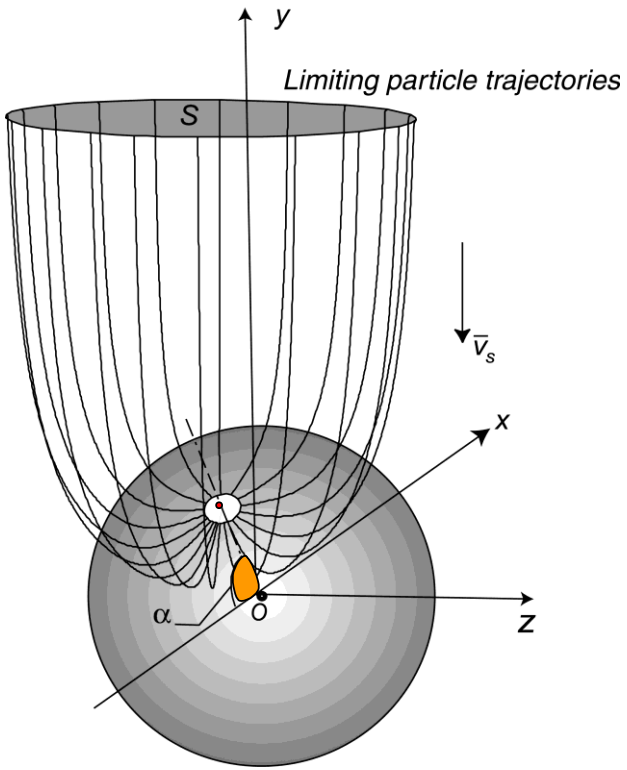

α=π/2

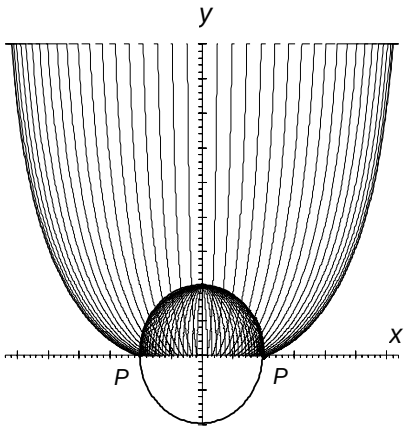

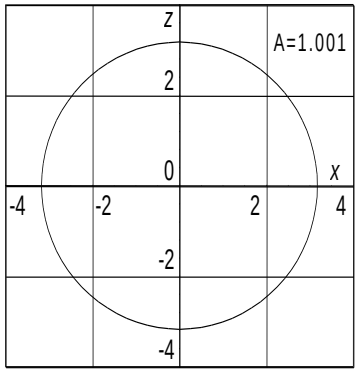

α=0

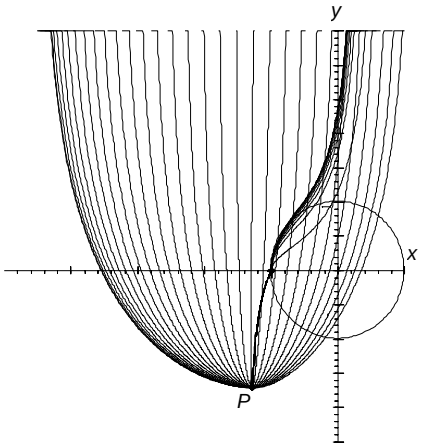

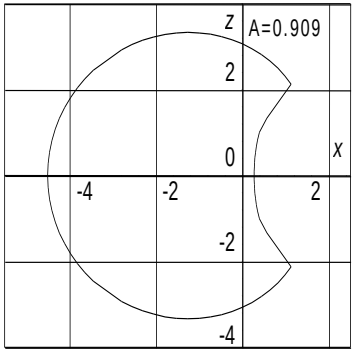

α=- π /2

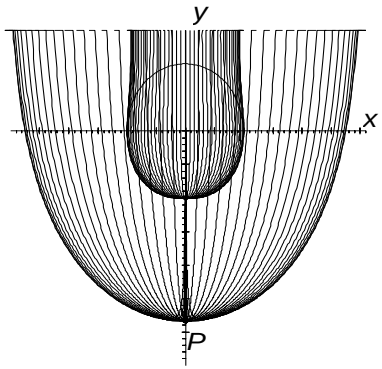

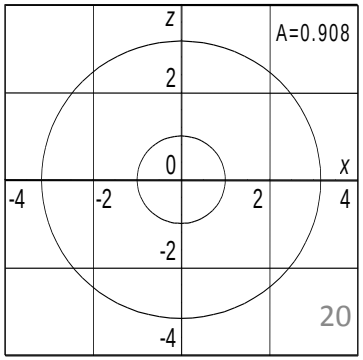

$\alpha=\pi/2$

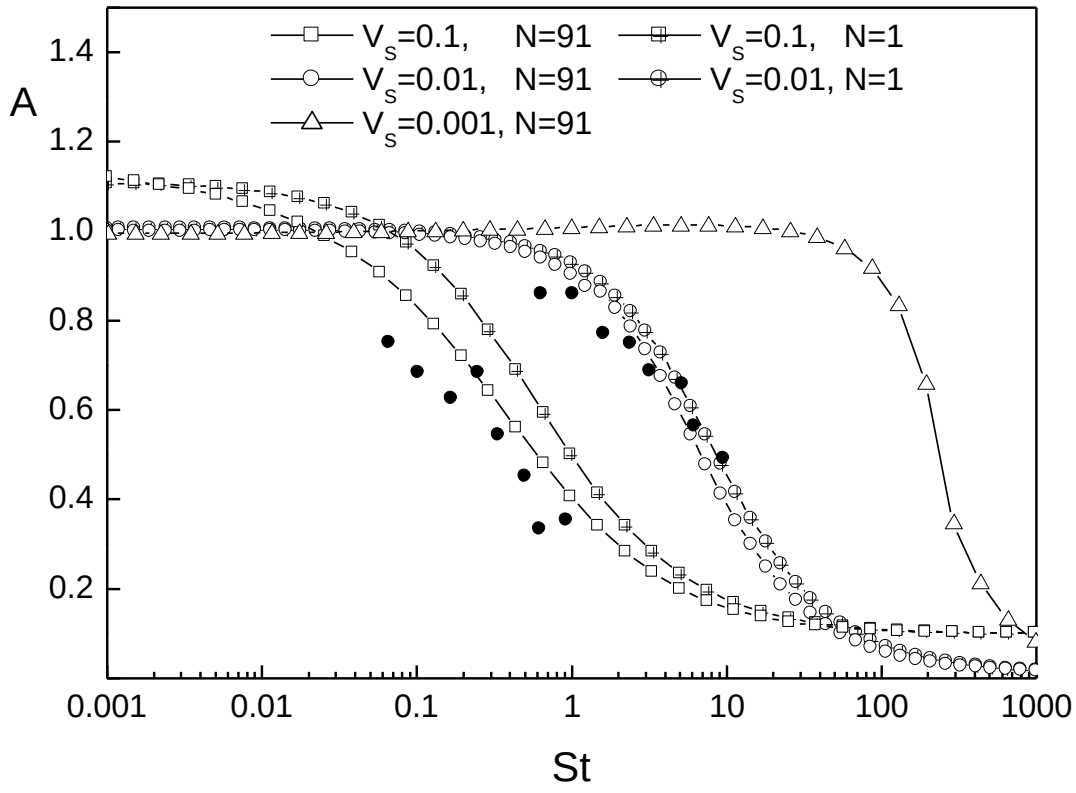

$A(St_c)$ для Vs=0.1 и 0.01

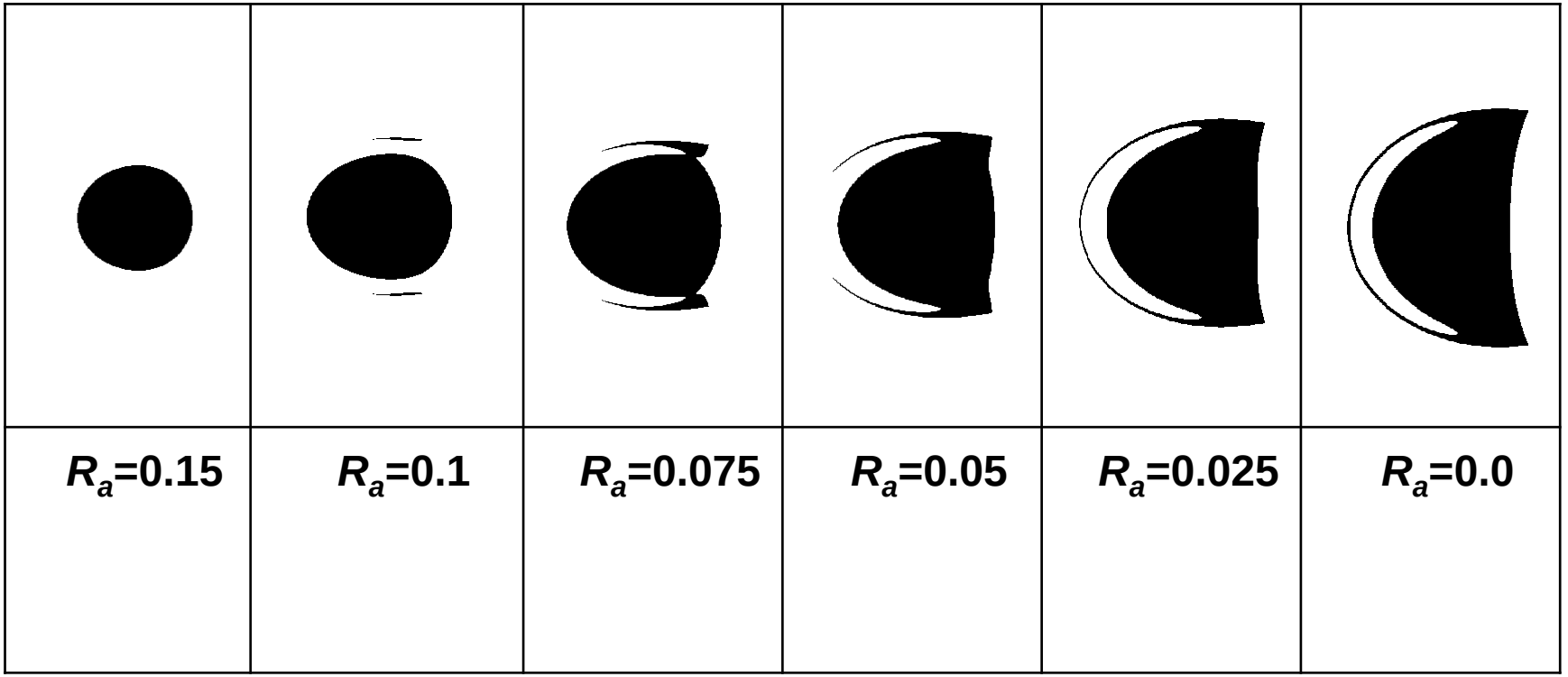

Fig.3. Aspirated particles area at St=1 and various R_c=0.1.

Approximate formula for aspiration efficiency of spherical sampler oriented horizontally

Levin (1961) approximate formula for aspiration efficiency of point sink

Su and Vincent (2004) formula for aspiration efficiency of spherical sampler oriented vertically downward and upward

$$A = 1 + \alpha k + \beta k^2$$

$$k = \mathrm{St}(R_a^2 + R_c^2)^{3/4} << 1$$

α=-15.19, β=63.6 approximation of results of numerical calculations

Aspiration efficiency - Inhalation fraction

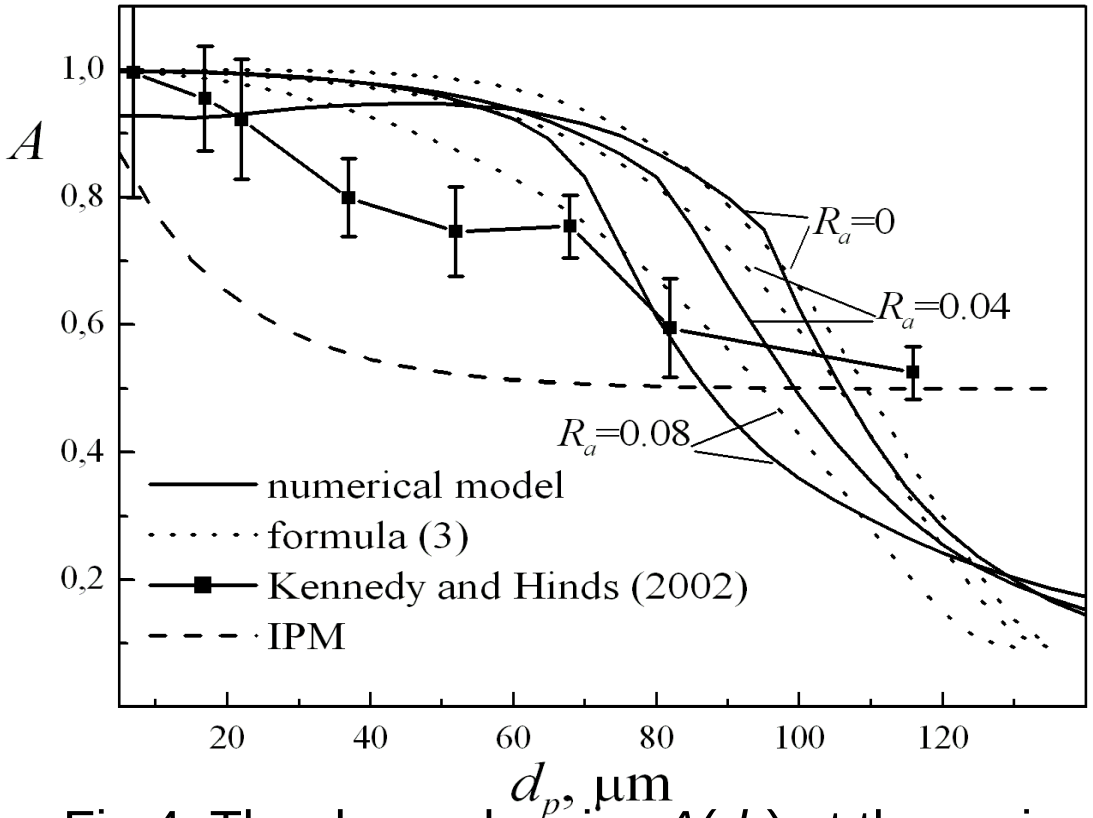

Fig.4. The dependencies $A(d_p)$ at the various R_a

$$\mathrm{IPM} = 0.5(1+\exp(-0.06d_p))$$

The criterion for inhalable particulate mass (IPM) from the American Conference of Governmental Industrial Hygienists (ACGIH)

Inhalation fraction study

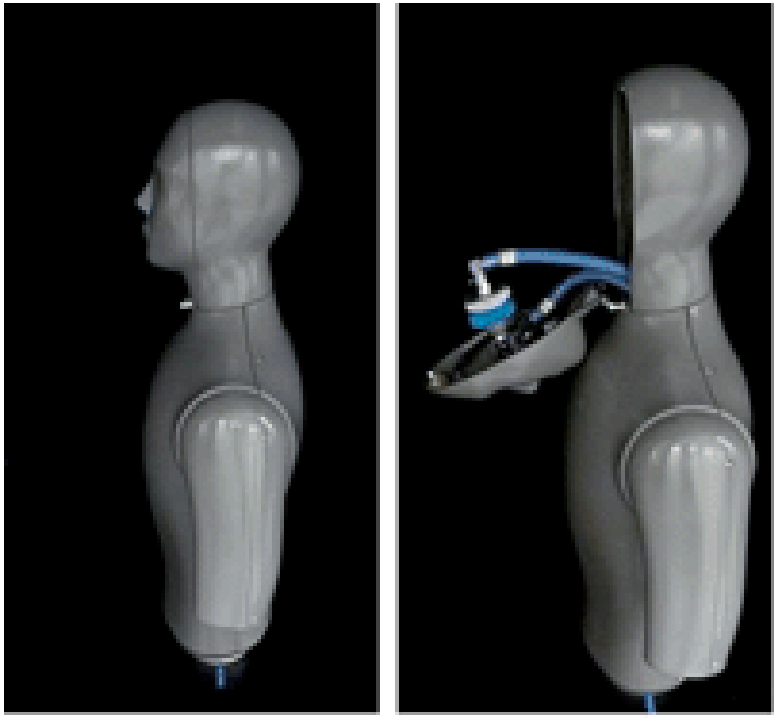

(a)

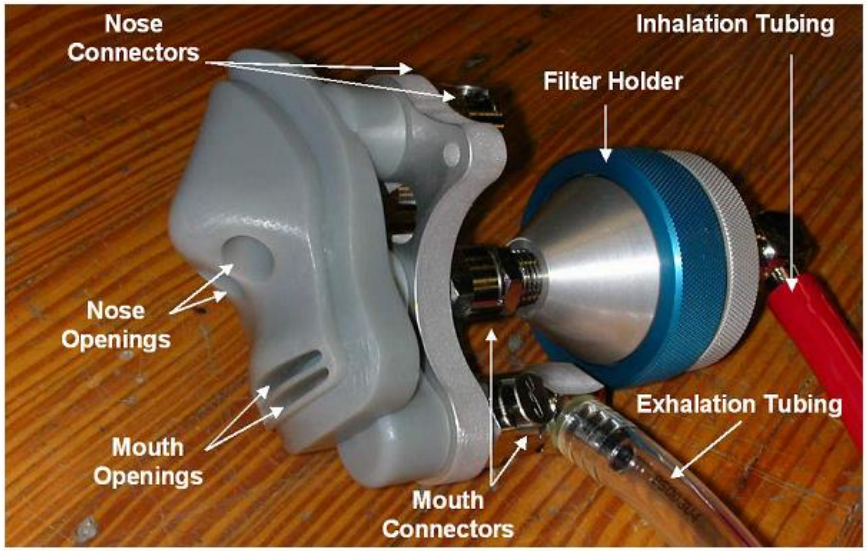

Figure 6.11 Mannequin breathing manifold with attached filter holder, indicating the various nose and mouth orifices as well as the separate internal tubing connections.

Darrah K. Schmees , Yi-Hsuan Wu and James H. Vincent

Experimental methods to determine inhalability and personal sampler performance for aerosols in ultra-low windspeed environments

J. Environ. Monit., 2008

CFD model of aerosol flow in the vicinity of manikin head

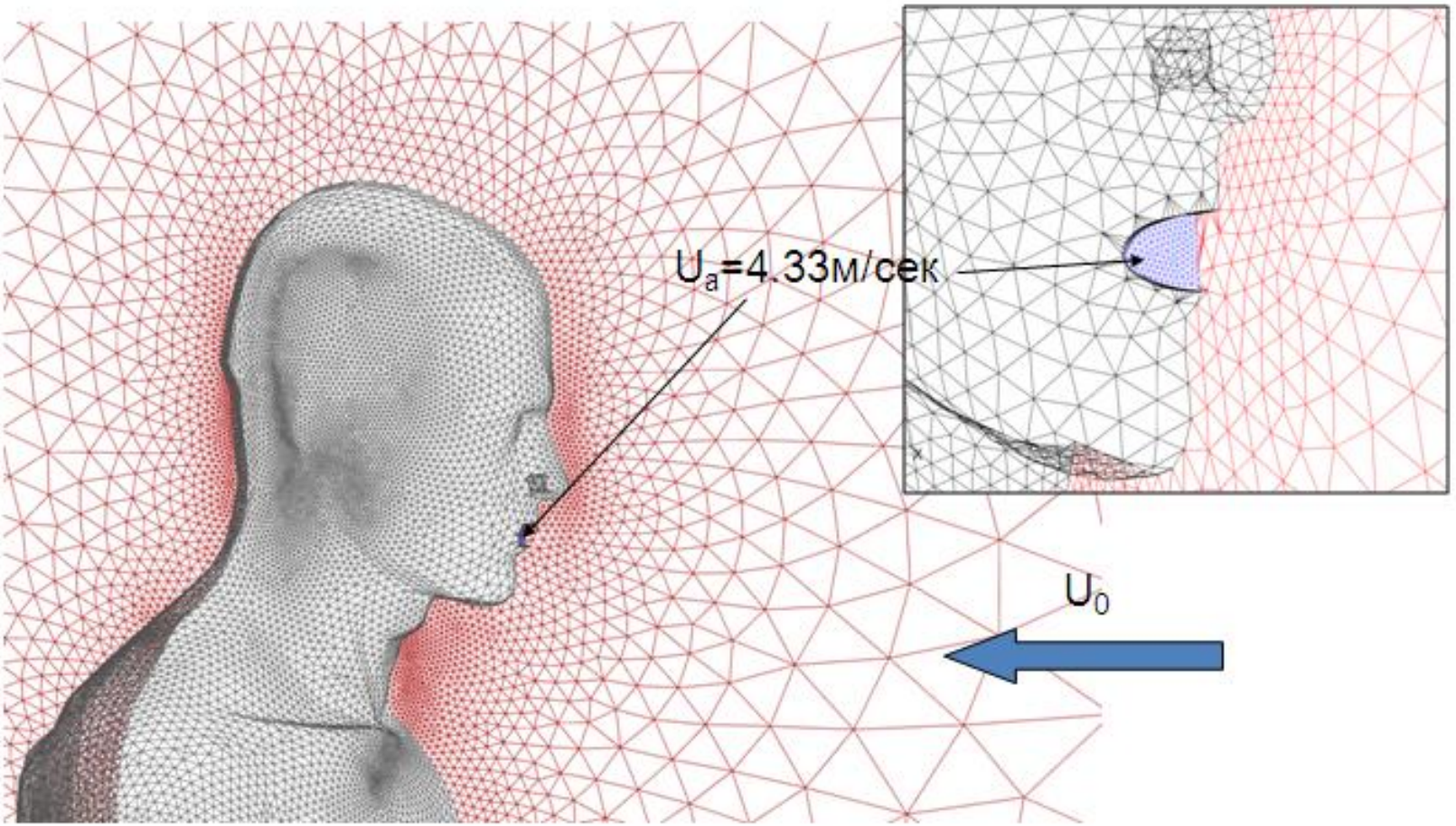

Meshing in the vicinity of manikin head

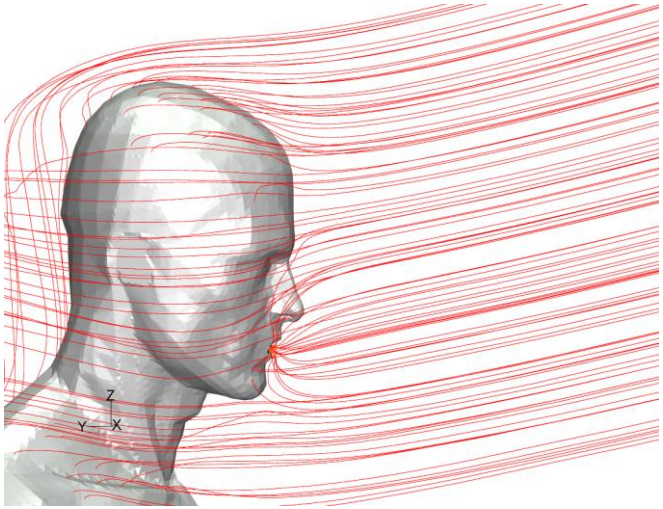

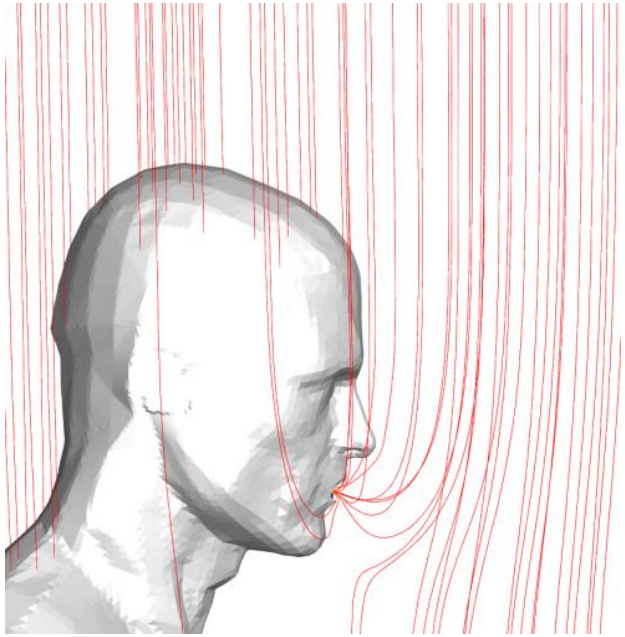

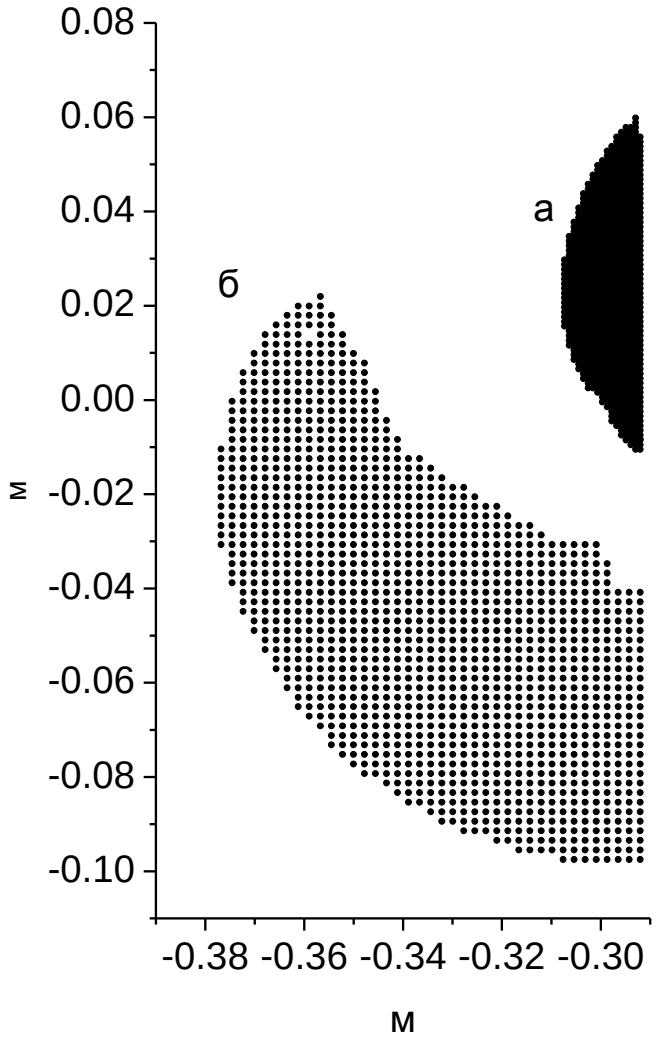

The trajectories of particles at d=37μm for two wind velocities: a-U_0=0.2 m/s, b - U_0=0

The area *Sp* of the aspirated particles

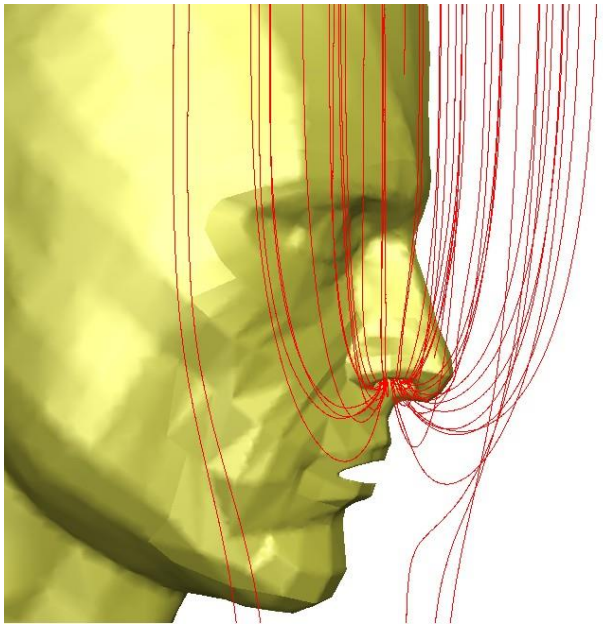

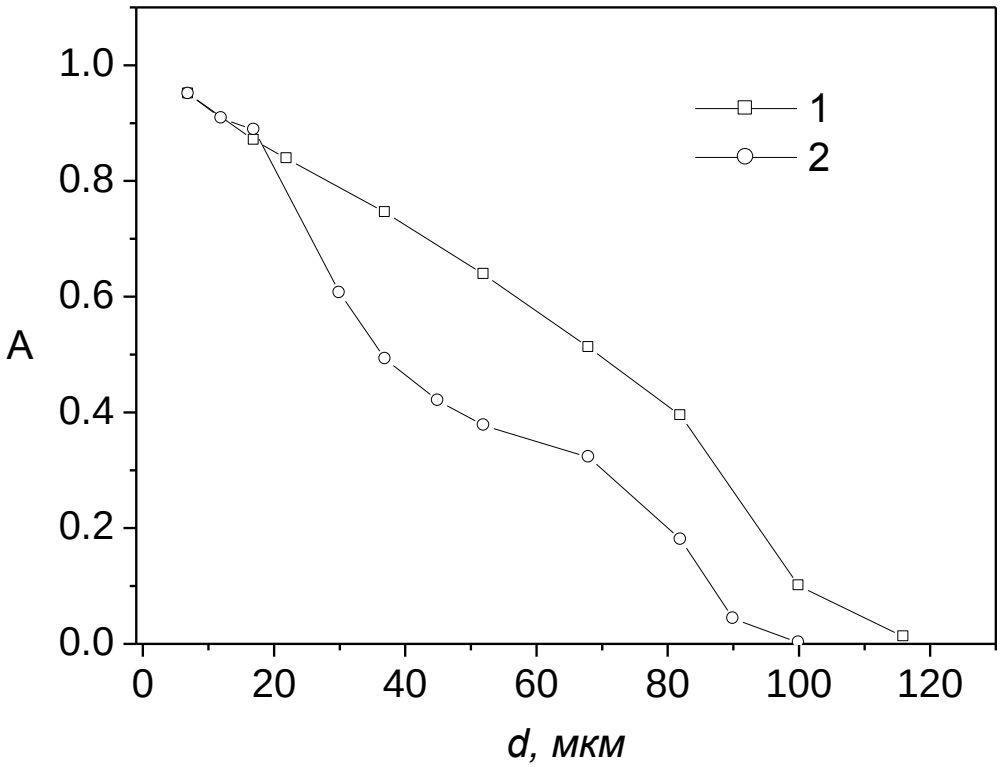

Inhalable fraction for breathing through mouth (1) and nose (2) in calm air

Facepiece filtering respirators (FFR) and surgical masks

Variety of respirator facepieces

Two pathways of particle penetration

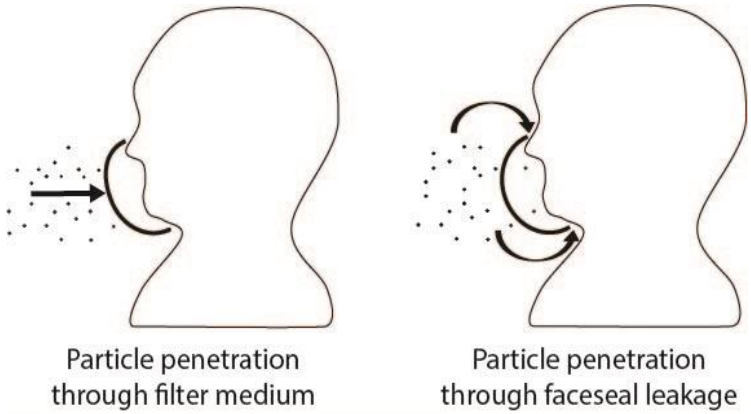

Performance evaluation on a manikin headform

Protection factor = C_{out}/C_{in}

Particle penetration = C_{in}/C_{out}

Studies of protection offered by FFRs and medical (surgical) masks: experiments and CFD modeling

Experimental (combining manikin-based and human study protocols):

Grinshpun et al. (2009). *J. Occup. Environ. Hyg*. 6: 593–603.

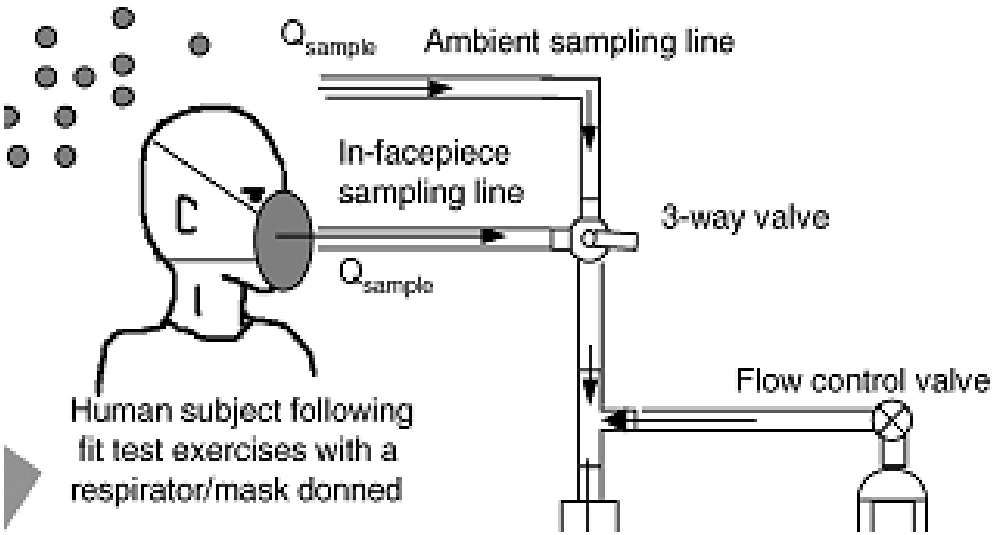

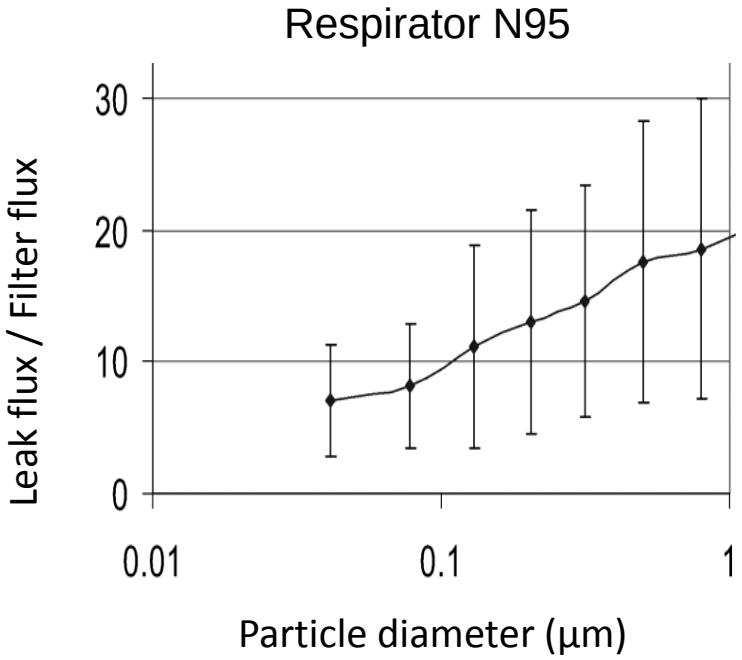

An idealized spherical sampler with porous layer

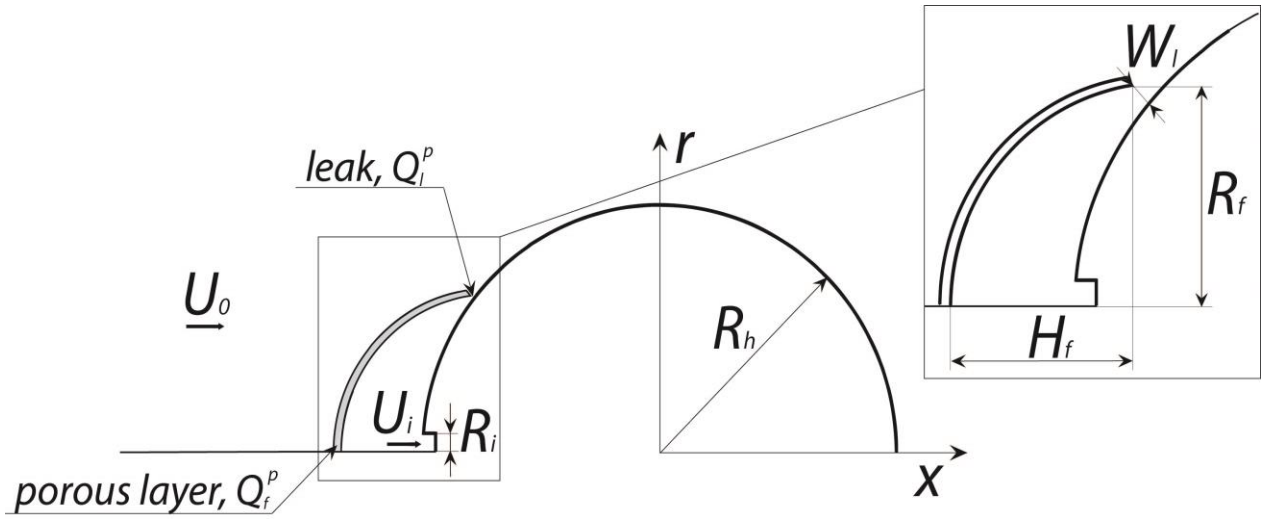

The fluid flow model: The air flow is assumed to be two-dimensional, laminar, incompressible and steady (**CFD code Fluent**)

$$\nabla \cdot \bar{u} = 0$$

$$\varepsilon^{-2}\bar{u} \cdot \nabla \bar{u} = -\nabla p + \frac{\mu}{\varepsilon}\Delta \bar{u} - b\frac{\mu}{k}\bar{u}$$

$\bar{u}$ – velocity vector
μ – viscosity
p – pressure
ε – porosity of the mask
k – permeability of porous material
b=1 porous zone (extended Brinkman equations)
b=0 free fluid zone (Navier-Stokes equations)

Penetration of aerosol particles through filter layer

$$\eta_f = \exp\left(-\frac{4\alpha E_f L}{\pi d_f (1-\alpha)}\right)$$

α = porous medium solidity
L = thickness of porous layer
d_f = fiber diameter

$$E_{fiber} = 1-(1-E_r)(1-E_d)(1-E_q)$$

E_r, E_d, E_q are the collection efficiencies of a single fiber due to interception, diffusion and electrostatic deposition

Interception (Payet *et al.*, 1992; Gougeon *et al.*, 1996)

$$E_r = 0.6\left(\frac{1-\alpha}{\mathrm{Ku}}\right)\frac{N_r^2}{(1+N_r)}c_r, \qquad N_r = d_p/d_{fiber}$$

$$c_r = \left(1+\frac{1.9996\mathrm{Kn}_{fiber}}{N_r}\right) \qquad \mathrm{Ku} = -0.5\ln\alpha - 0.75 + \alpha - 0.25\alpha^2$$

Diffusion (Payet *et al.*, 1992; Gougeon *et al.*, 1996)

$$E_d = 1.6\beta \mathrm{Pe}^{-2/3} c_d c_d^*$$

$$\beta = \left(\frac{1-\alpha}{\mathrm{Ku}}\right)^{1/3}, \qquad \mathrm{Pe} = U_f \cdot d_{fiber}/D$$

$$c_d = \left(1+0.388\mathrm{Kn}_{fiber}\beta\mathrm{Pe}^{1/3}\right), \qquad D = k_b T C_c / 3\pi\mu d_p$$

$$c_d^* = \left(1+1.6\beta\mathrm{Pe}^{-2/3}c_d\right)^{-1} \qquad \mathrm{Kn}_{fiber} = \lambda / d_{fiber}$$

Electrostatic deposition (Kanaoka *et al.*, 1987)

$$E_q = 0.06 N_{Q0}^{2/5}$$

$$N_{Q0} = \frac{C_c q^2 d_p^2 (\varepsilon_p - 1)}{3\pi^2 \varepsilon_0 \mu d_{fiber}^3 U_f (\varepsilon_p + 2)}$$

q = the charge density of a single fiber

ε_p = the relative permittivity of the fiber

$\varepsilon_0 = 8.85\cdot10^{-12}$ F m^{-1} = the vacuum permittivity.

Fitting the porous layer permeability to the experimental curves $\eta_f(d_p)$ from Rengasamy and Eimer (2012)

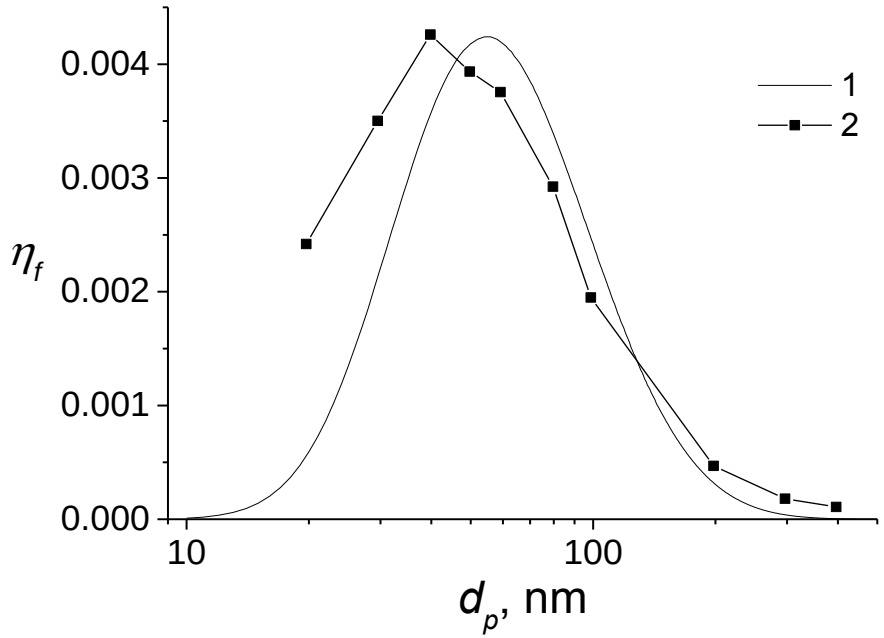

The particle penetration through the filter $\eta_f(d_p)$ at Q_i = 30 l min^{-1}
1 –approximated formulas d_{fiber} = 10.07 µm, α=0.069, L=3 mm
2 – experimental values from Rengasamy and Eimer (2012).

Kozeny-Carman formula:

$$k = \frac{\varepsilon^3 d_{fiber}^2}{180(1-\varepsilon)^2}$$

Permeability used for calculations:

$$k = 9.55 \cdot 10^{-11}\ \mathrm{m}^2$$

Parameters and conditions used in the modeling

European FFP2 and American N95 respirators: S_f = 0.0158–0.0255 m^2 (Roberge *et al*., 2010).

Present spherical model:

R_i = 0.007 m (S_i = 0.000154 m^2)

R_h = 0.09 m

spherical segment with
a height of H_f = 0.05 m and
a base radius of R_f = 0.057 m

$$S_f = 0.018\ m^2$$

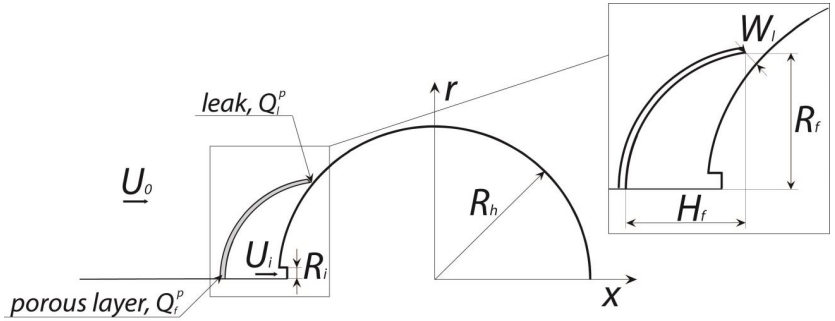

Q_i =8, 30, 40, and 85 l min $^{-1}$ correspond to U_i = 0.870, 3.25, 4.33, and 9.20 m s^{-1}

Q_i = 6–8 l min^{-1} (rest), 30 and to 40 l min^{-1} (moderate work load), and 85 l min^{-1} (heavy work load)

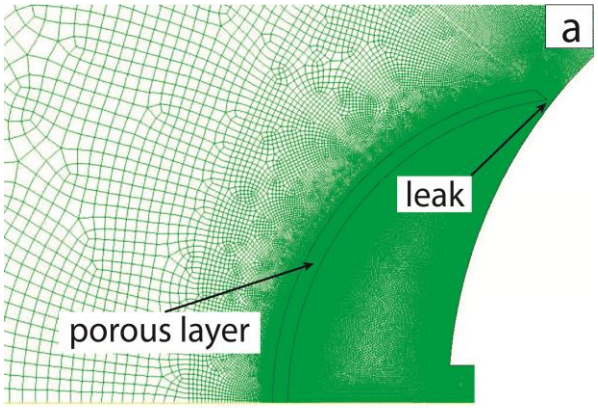

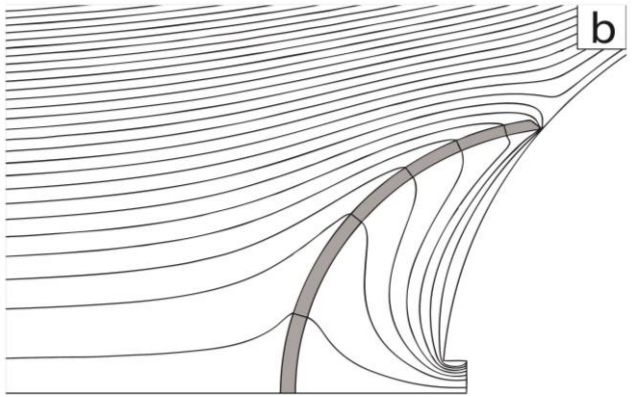

The unstructured grid near the inhalation orifice (*a*) and the streamlines for the flow through the porous layer (*b*). Calculated for W_l = 1mm, Q_i = 30 l min^{-1}, and k = 9.55·10^{-11} m^2.

Comparison to the experimental data of Rengasamy and Eimer (2012)

Rengasamy, S., and Eimer, B.C. (2012). Nanoparticle penetration through filter media and leakage through face seal interface of N95 filtering facepiece respirators. *Ann. Occup. Hyg*. 56: 568–580.

A correction factor to fit two circular and annular shape holes areas ~2

Chen, C.C. and Willeke, K. (1992). Characteristics of face seal leakage in filtering facepieces. *Am. Ind. Hyg. Assoc. J.* 53: 533–539.

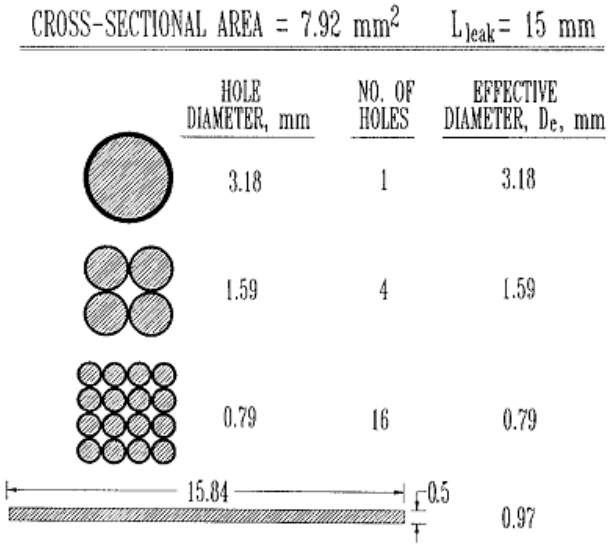

FIGURE 1. Leak sizes used in study

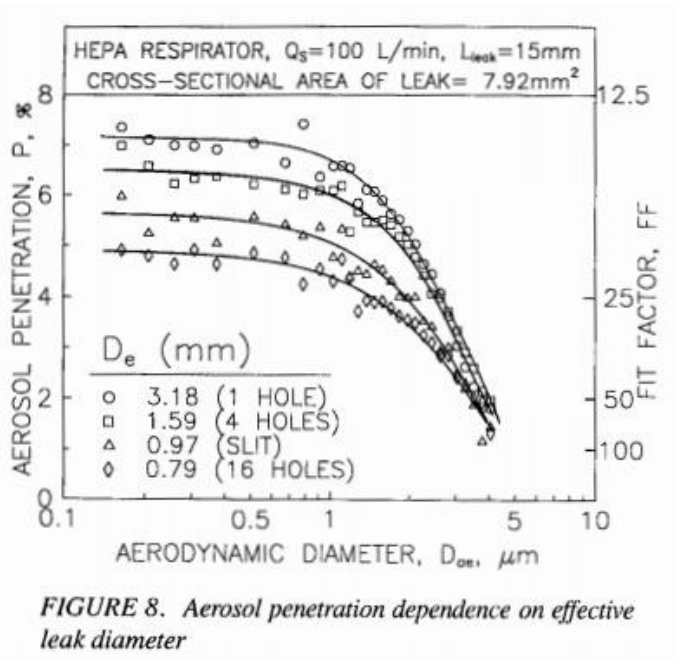

FIGURE 8. Aerosol penetration dependence on effective leak diameter

MODELING RESULTS:

$TIL = f(S_l/S_f)$ at d_p = 50 nm (a), 100 nm (b), and 1 μm (c) for different inhalation flow rates

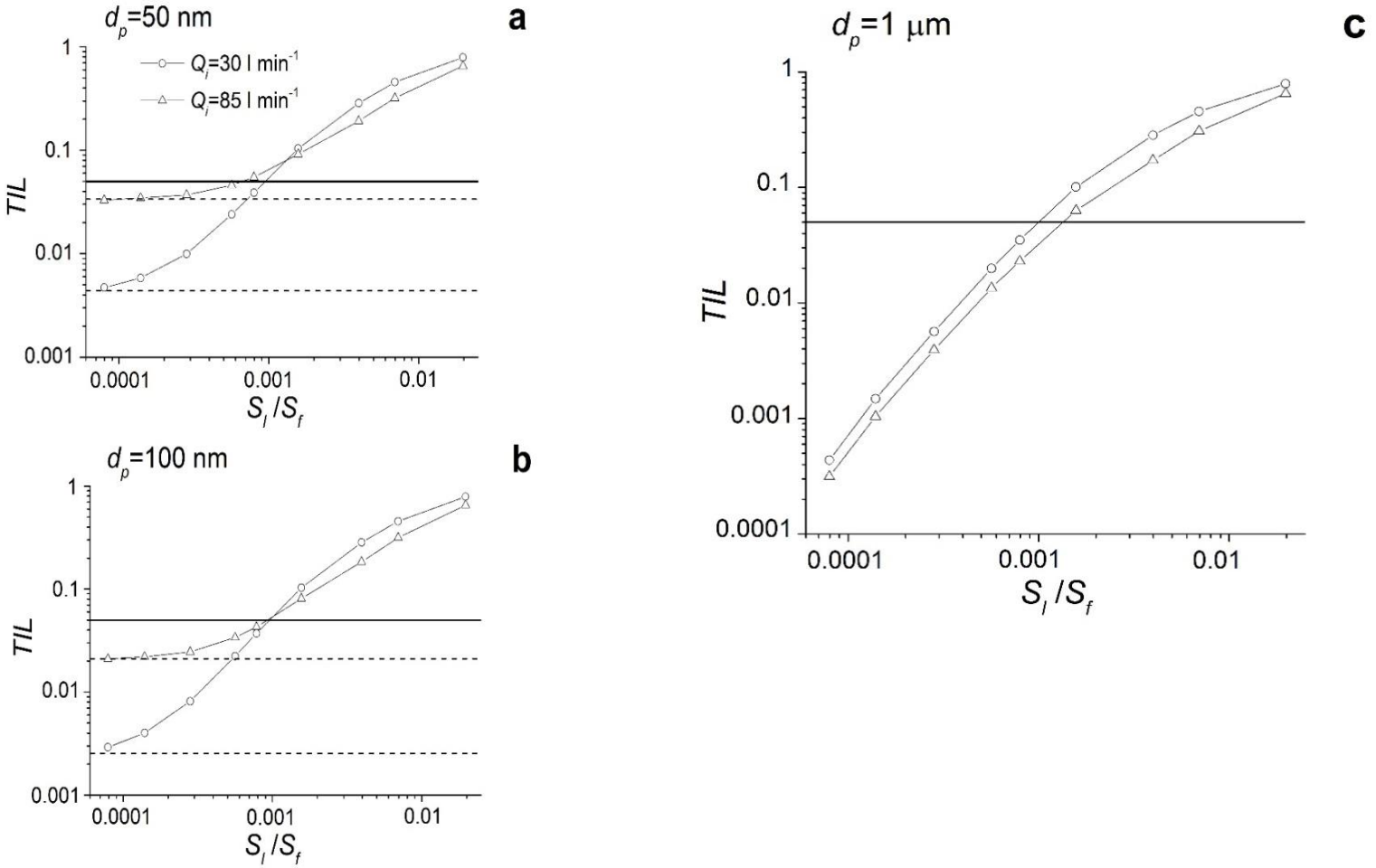

Solid lines represent the target value for an N95 (*TIL*=0.05).

Dotted lines represent a "perfect fit" respirator (with no faceseal leakage).

NUMERICAL STUDY OF GROWING DROPLETS DYNAMICS IN UNSTEADY THERMAL CONVECTION FLOW

S.K. ZARIPOV , R.S.Galeev , W.Holländer. Numerical study of dynamics of growing droplets in Kelvin spectrometer. Abstracts of European Aerosol Conference-2007, Salzburg, T12A033.

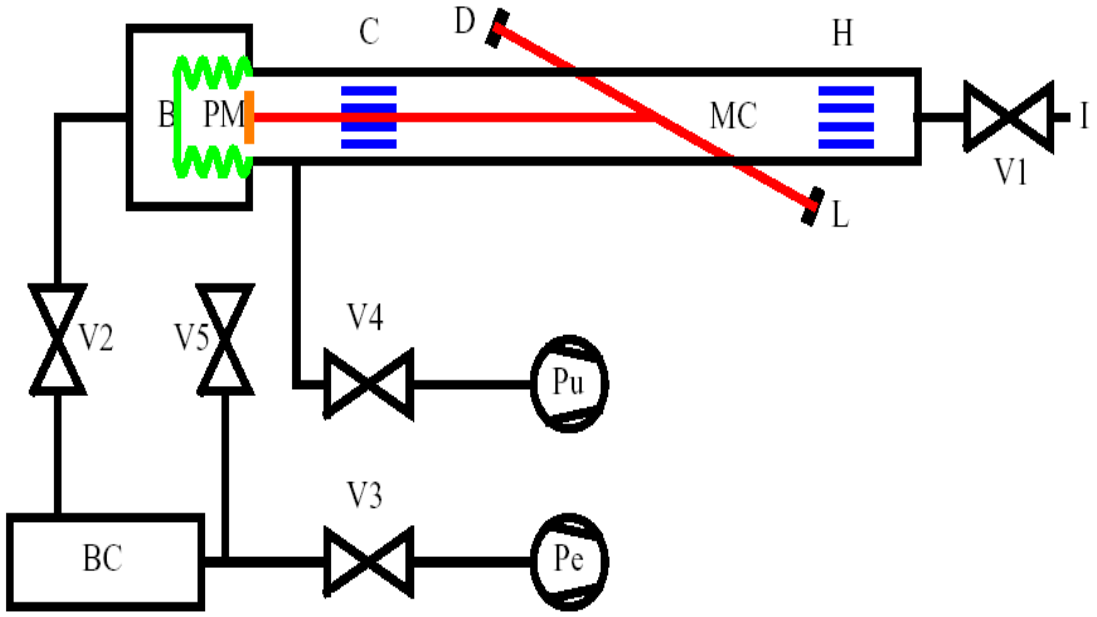

▲ **Figure 1.** The new design. The main change consists in enclosing a fixed air mass in the measuring chamber MC allowing a series of measurements taken at different supersaturations. Transmittance is measured following the intensity arriving at D, and light scattered under 30° is detected by the photomultiplier PM.

Fig.8. Time evolution of the temperature distribution in the cross section of the horizontal cylinder

$$T_{\infty}(\overline{r}_p, t)$$

1s

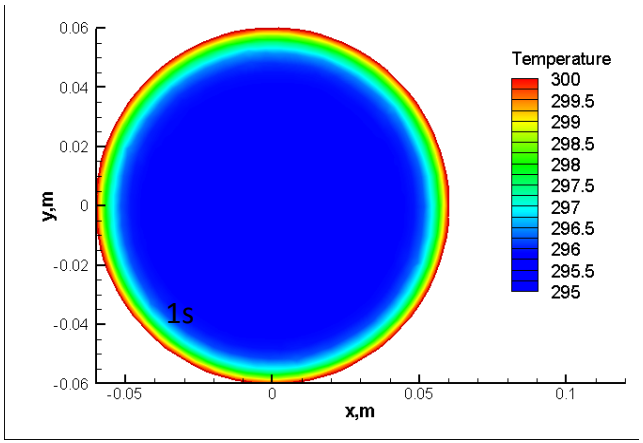

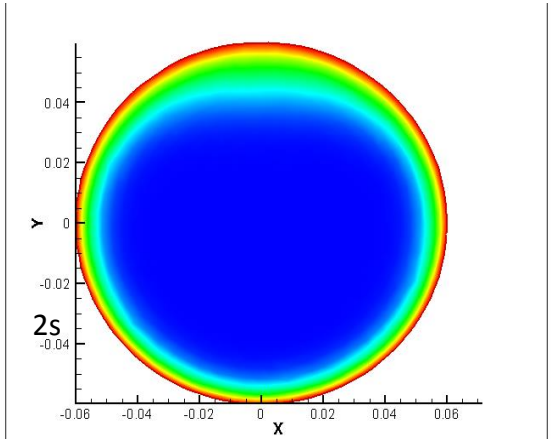

2s

5s

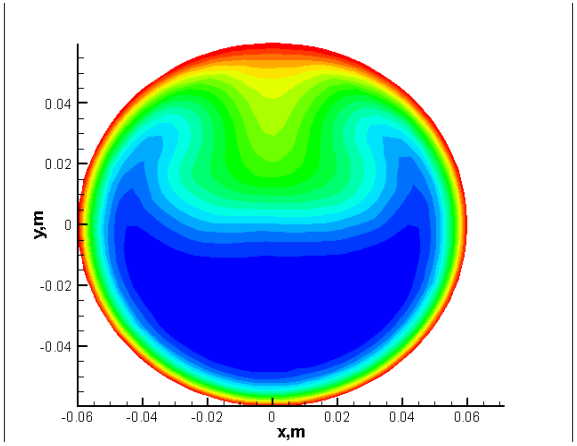

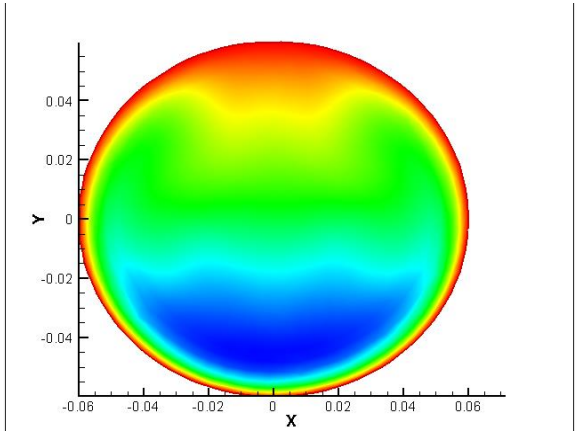

10s

Fig.7. Time evolution of the contours of velocity magnitude in the cross section of the horizontal cylinder

$\bar{U}(\bar{r}_p, t)$

1s

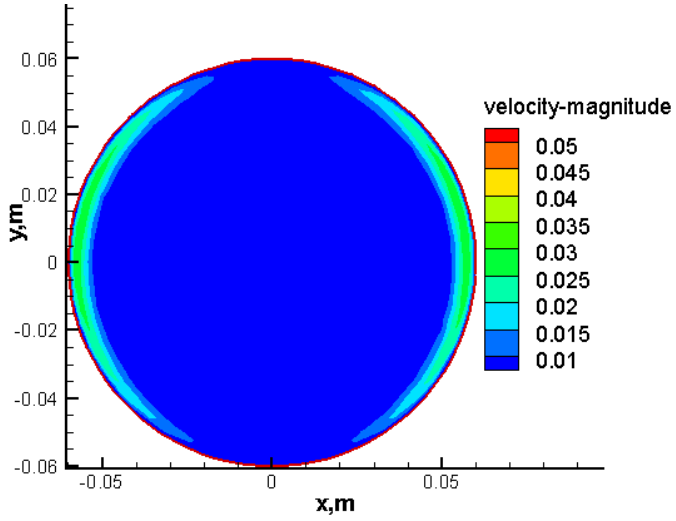

2s

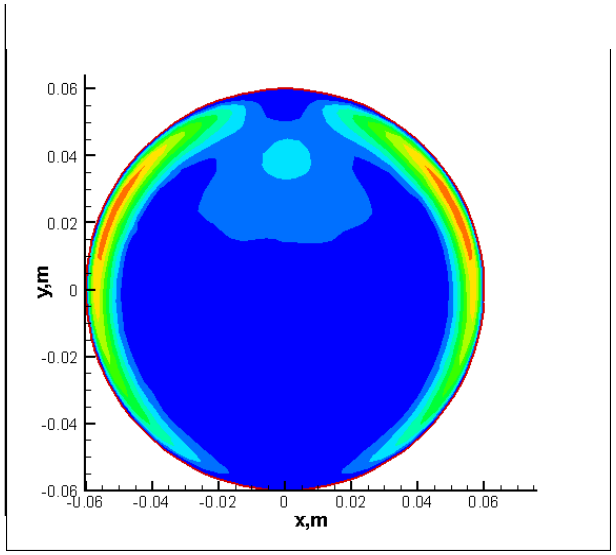

5s

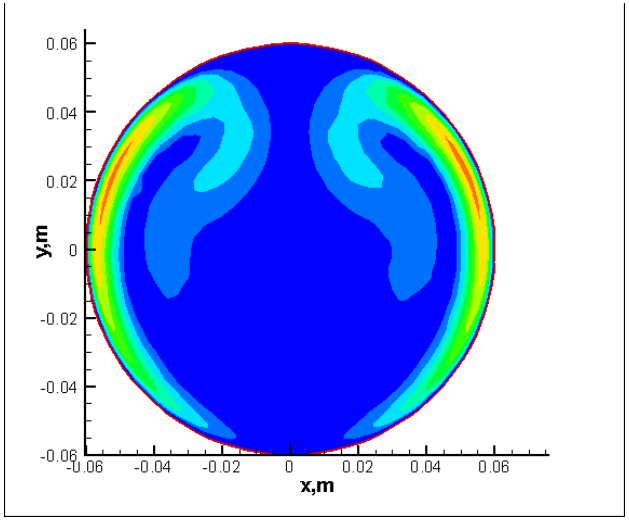

10s

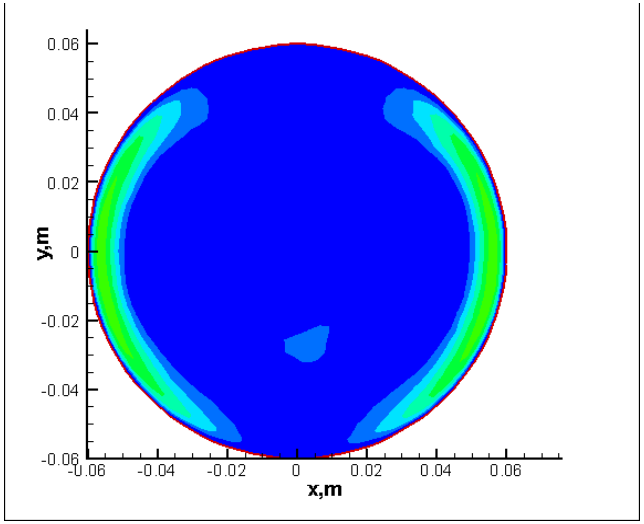

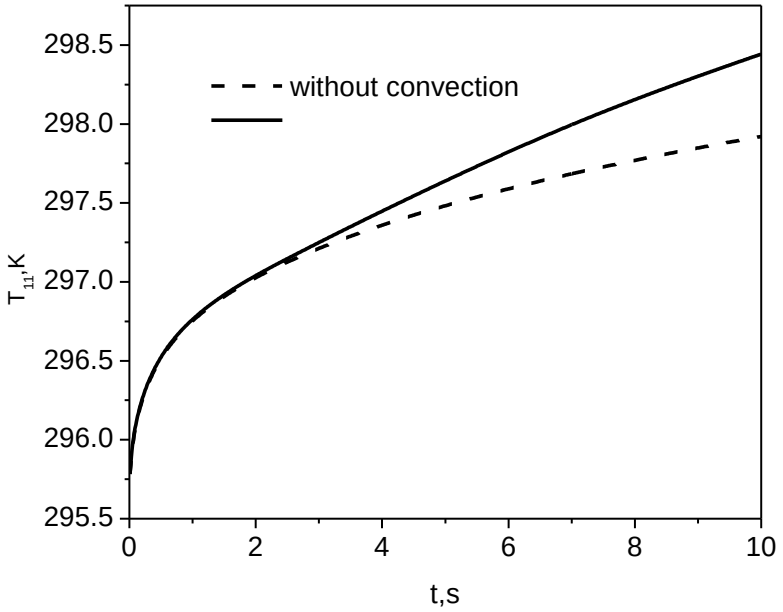

Fig.7. Average gas temperature with and without convection influence

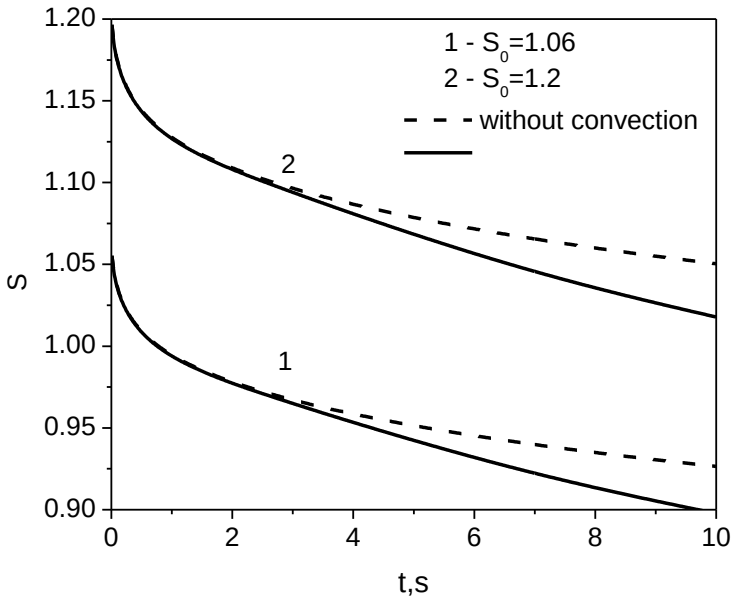

Fig.8. The saturation based on the average temperature gas temperature with and without convection influence

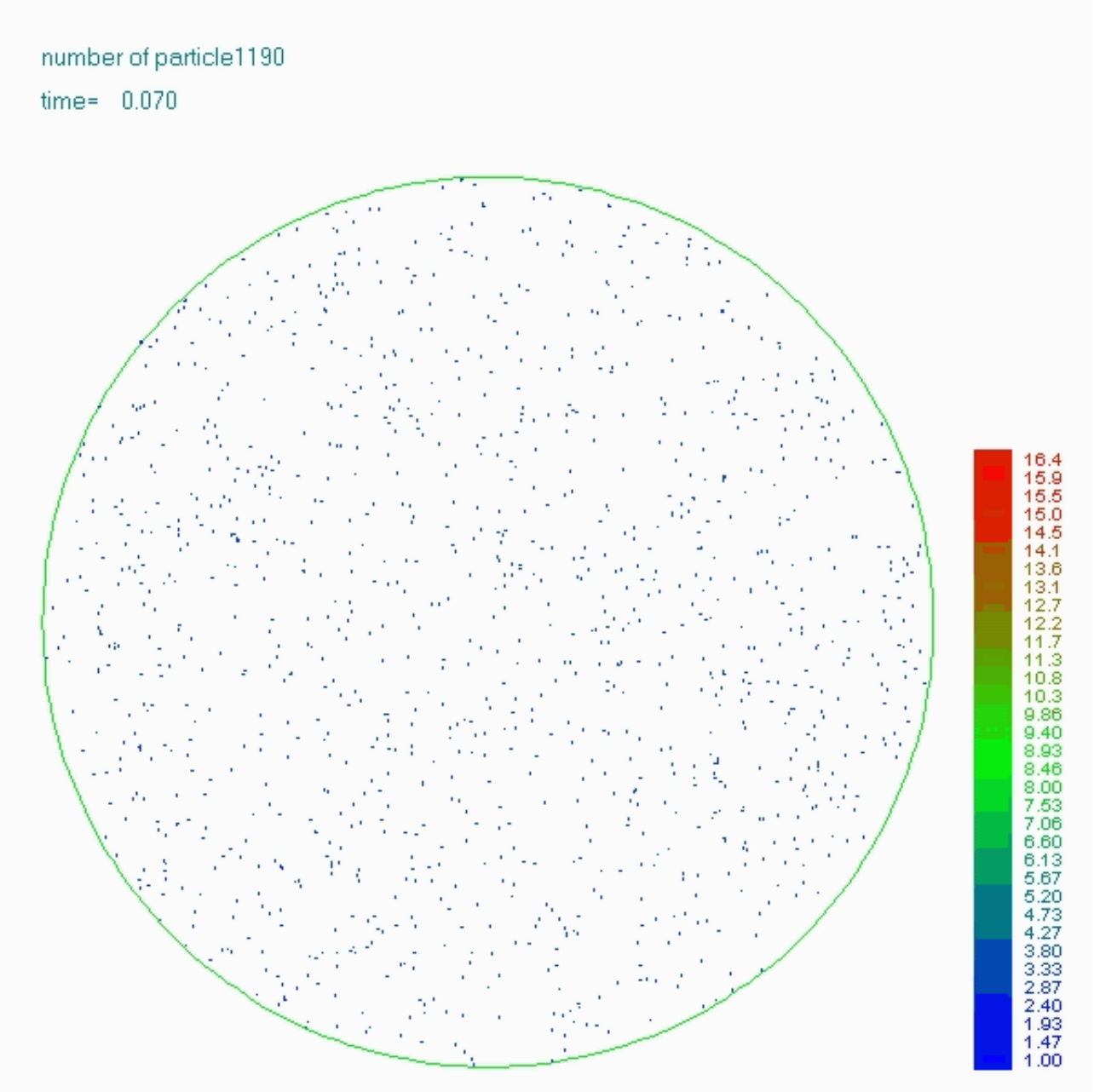
number of particle1190
time= 0.070
16.4
15.9
15.5
15.0
14.5
14.1
13.6
13.1
12.7
12.2
11.7
11.3
10.8
10.3
9.86
9.40
8.93
8.46
8.00
7.53
7.06
6.60
6.13
5.67
5.20
4.73
4.27
3.80
3.33
2.87
2.40
1.93
1.47
1.00

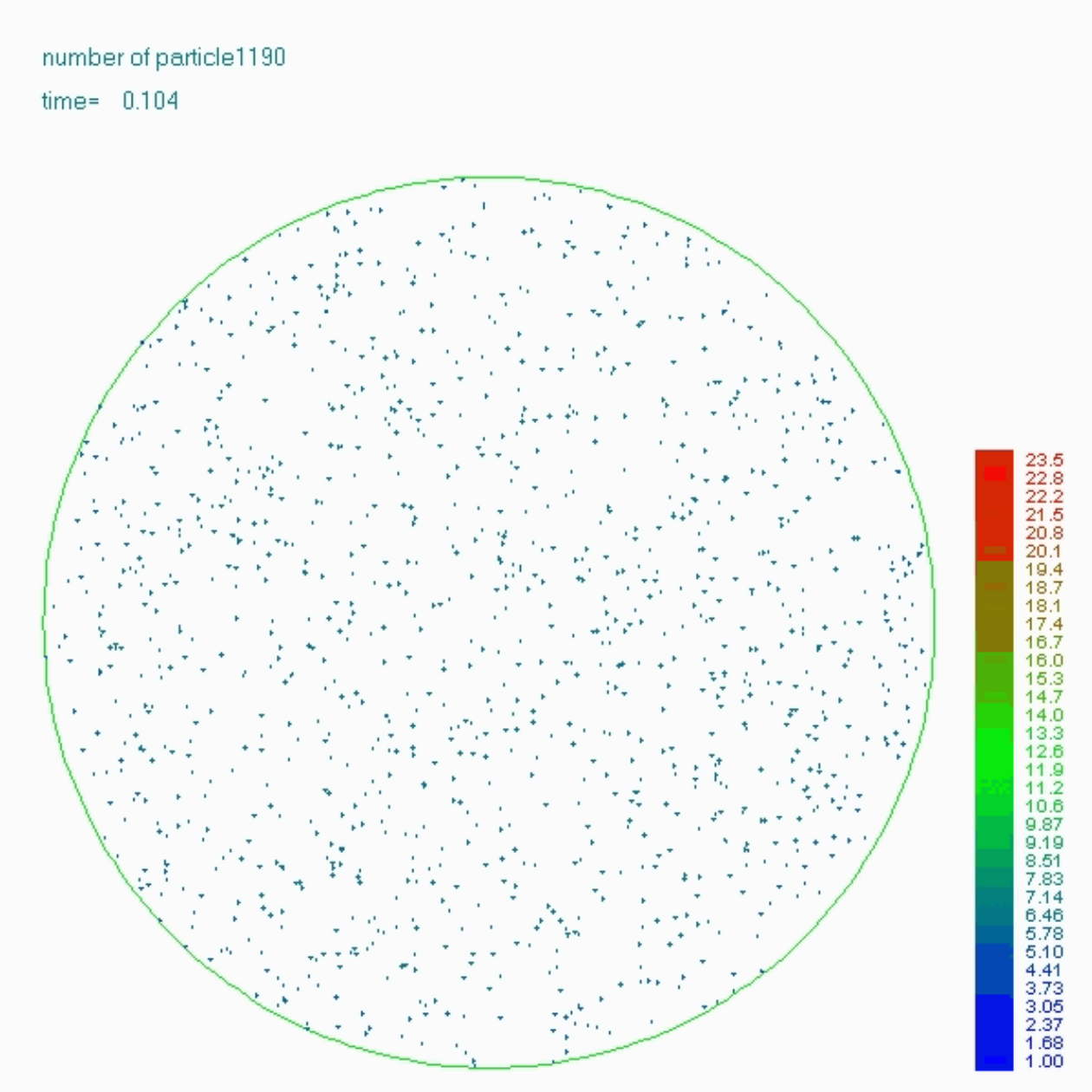
number of particle1190
time= 0.104
23.5
22.8
22.2
21.5
20.8
20.1
19.4
18.7
18.1
17.4
16.7
16.0
15.3
14.7
14.0
13.3
12.6
11.9
11.2
10.6
9.87
9.19
8.51
7.83
7.14
6.46
5.78
5.10
4.41
3.73
3.05
2.37
1.68
1.00

Fig.14. The mass density of condensing vapor on all droplets for N=1000 cm-3 and various initial saturations

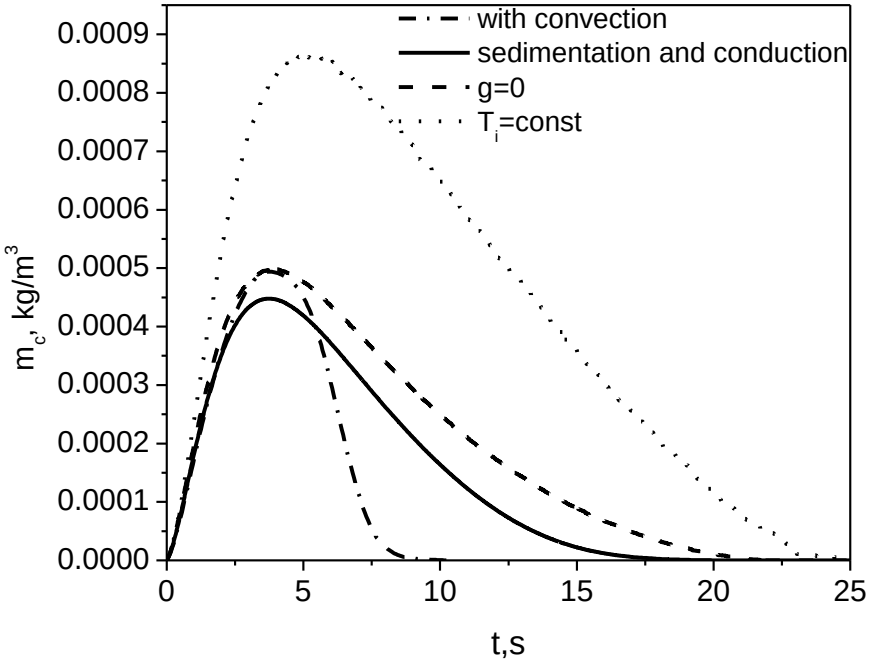

g=9.81m/s

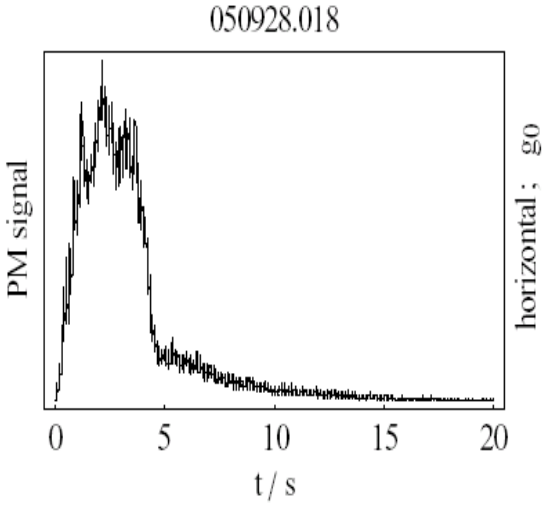

g=0

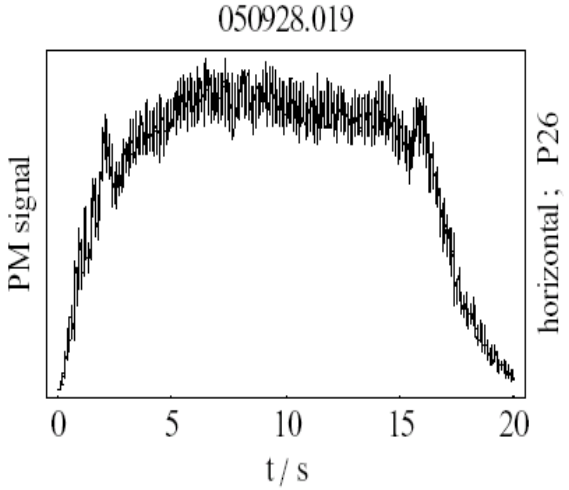

Aerosol filtration

Transport equations for charged particles

$C(\bar{r},t)$ - particle concentration

$$J_D = -D\,\nabla \cdot C$$ Diffusion flux

$$\bar{J}_u = C\bar{U}$$ convective transport

$$\bar{J} = qb\bar{E}C$$ transport due to electrostatic motion

$$\frac{\partial C}{\partial t} = D\nabla^2 C - \bar{U}\nabla C - qb\nabla\cdot(C\bar{E})$$

$$\bar{E} = -\nabla F \qquad \Delta F = -\frac{qC}{\varepsilon_0}$$

q - charge quantity

$$\bar{u}\cdot\nabla c - \mathrm{Pe}^{-1}\Delta c - \beta\nabla\cdot(c\nabla\varphi) = 0$$

$$\Delta\varphi = -c,$$

$$\bar{u} = \bar{U}/\bar{U}_0,\ Pe = R_c\bar{U}_0/D,\ \varphi = F\varepsilon_0/qC_0,\ c = C/C_0,\ \beta = q^2C_0B/R_cU_0\varepsilon_0,\ C_0$$

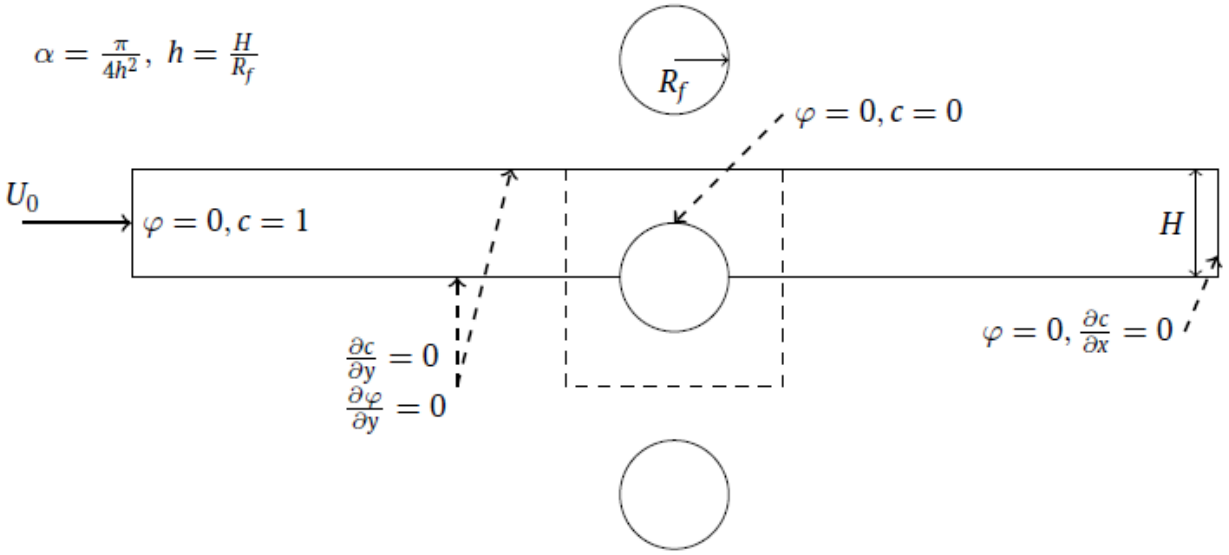
$\alpha = \frac{\pi}{4h^2}$, $h = \frac{H}{R_f}$
R_f
$\varphi = 0, c = 0$
U_0
$\varphi = 0, c = 1$
H
$\frac{\partial c}{\partial y} = 0$
$\frac{\partial \varphi}{\partial y} = 0$
$\varphi = 0, \frac{\partial c}{\partial x} = 0$

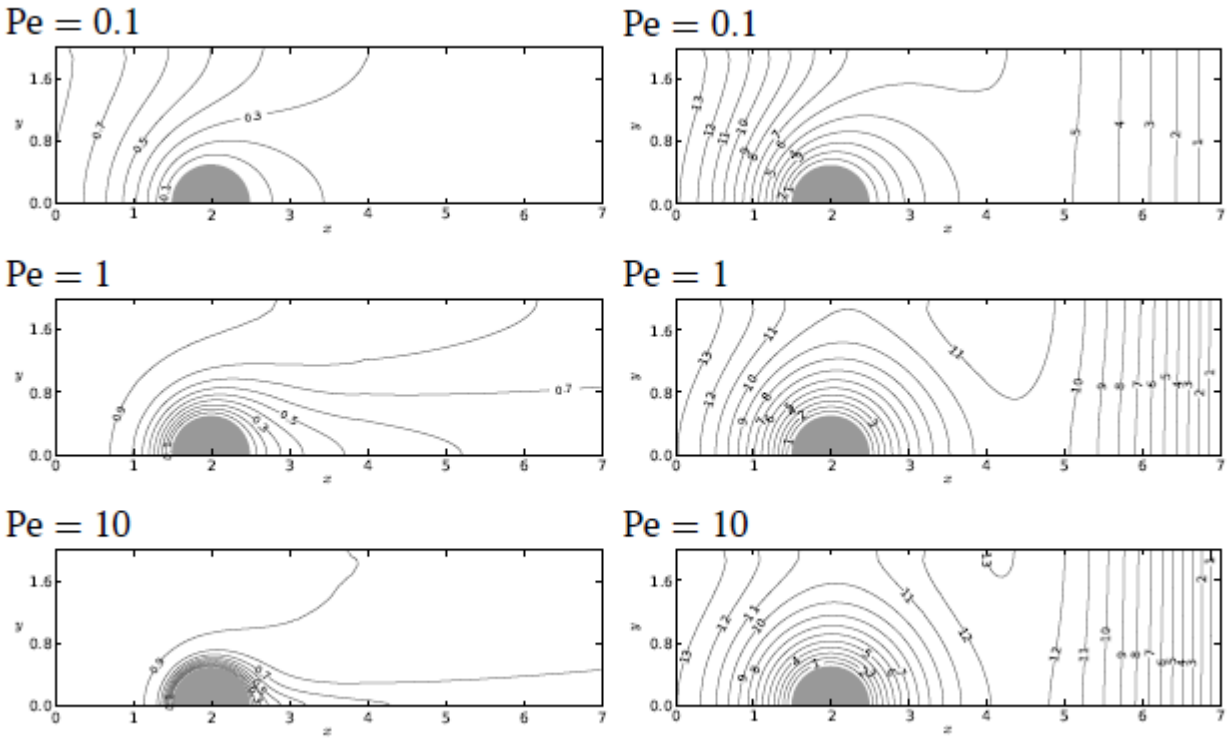
Pe = 0.1
Pe = 0.1
Pe = 1
Pe = 1
Pe = 10
Pe = 10

Deposition efficiency

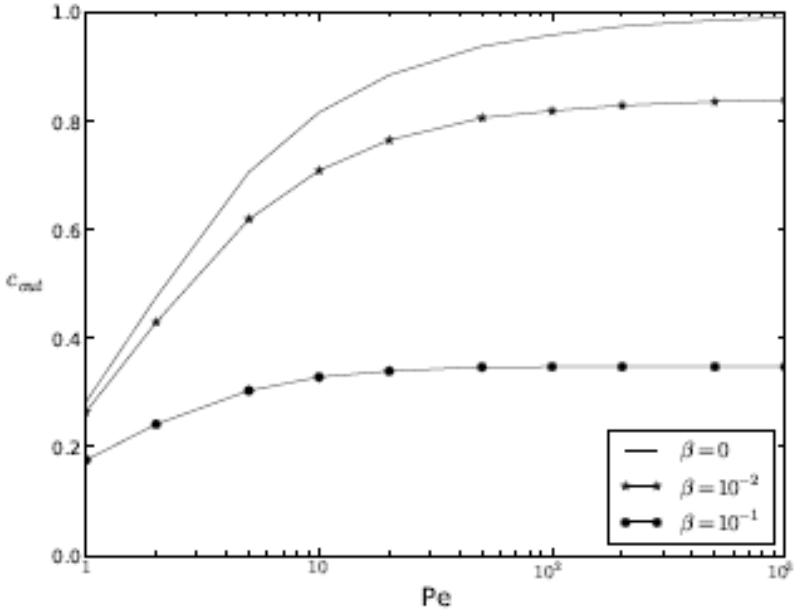

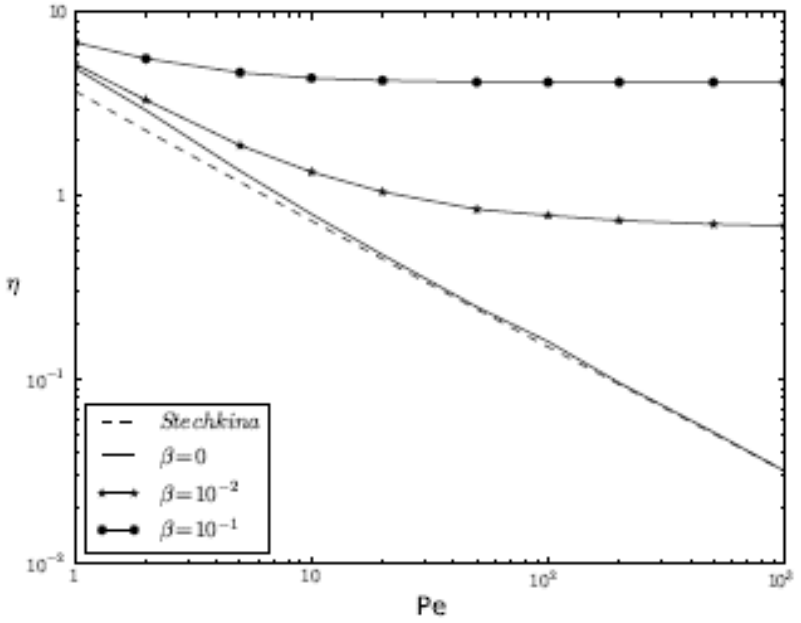

Aerosol deposition on the porous cylinder

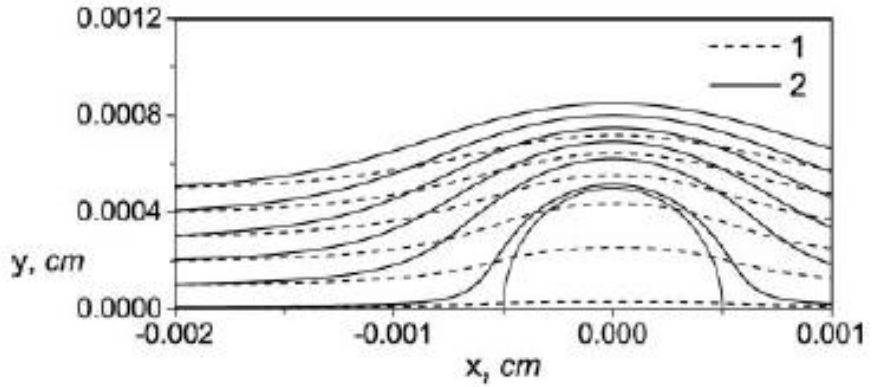

FIG. 4. Streamlines from numerical model $\alpha = 0.05$: (1) $\mathrm{Da} = 10^{-1}$, (2) $\mathrm{Da} = 10^{-3}$.

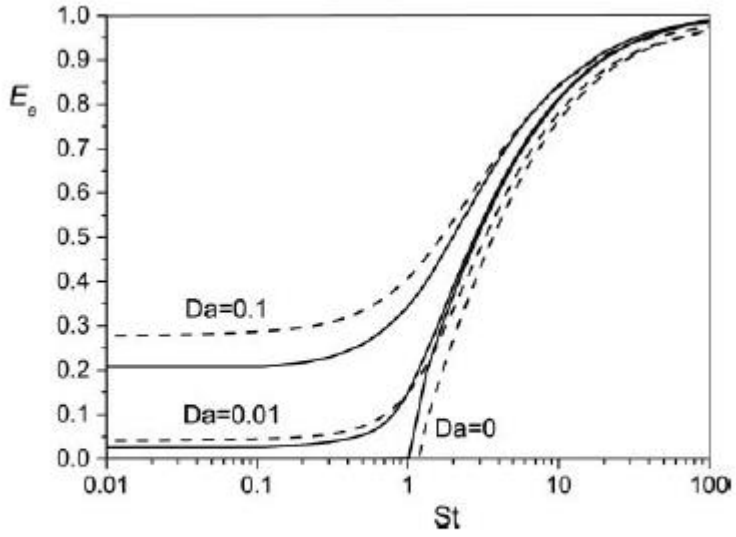

FIG. 5. The dependence of $E_e(\mathrm{St})$ at $\alpha = 0.05$. Solid lines—analytical model (10,17), dashed lines—CFD calculations.

Deposition of aerosol particles in dense array of spheres

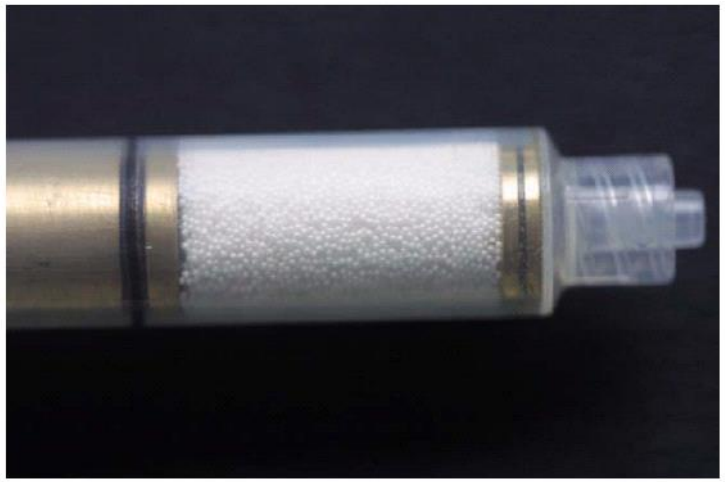

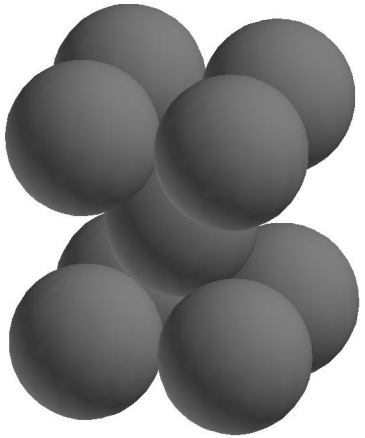

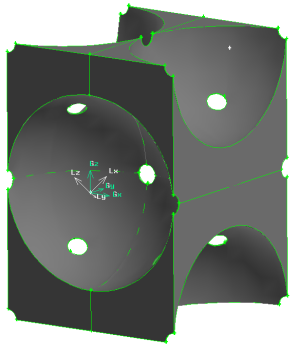

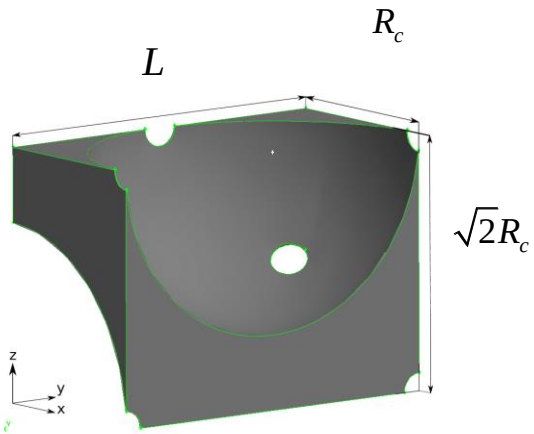

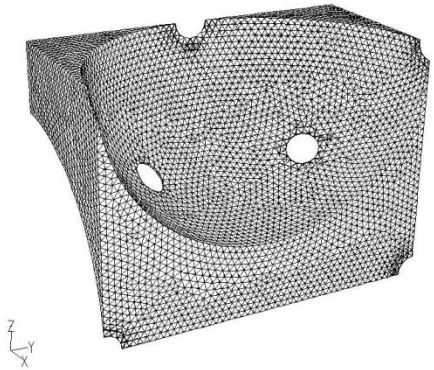

Particle motion equations

$$m\frac{d\bar{v}}{dt} = m\beta\left(\bar{u} - \bar{v}\right) + m\bar{A}\left(t\right) + m\bar{g} + \bar{F}_e$$

Inertial deposition

Gravitational deposition

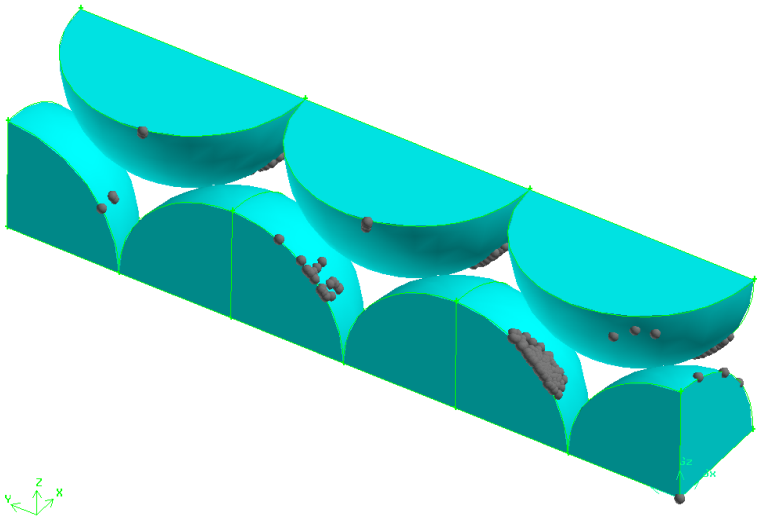

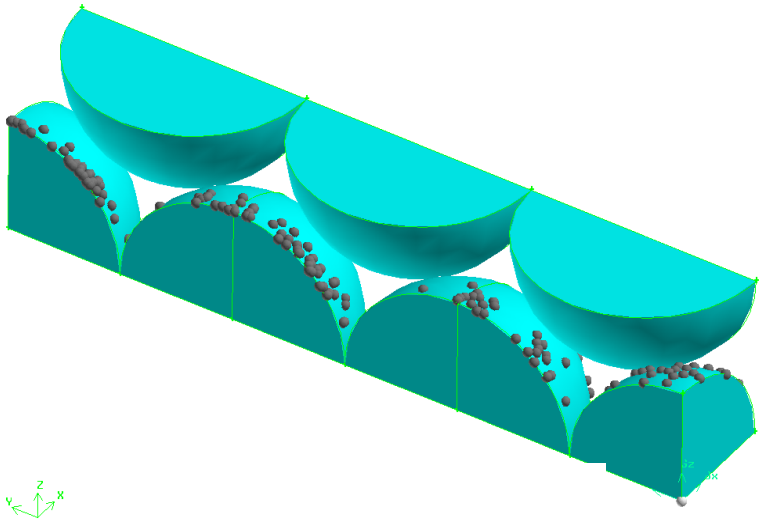

d=10 μm

d=5 μm

Deposition of charged particles for two numbers of elementary units of charge

d=0.6 μm

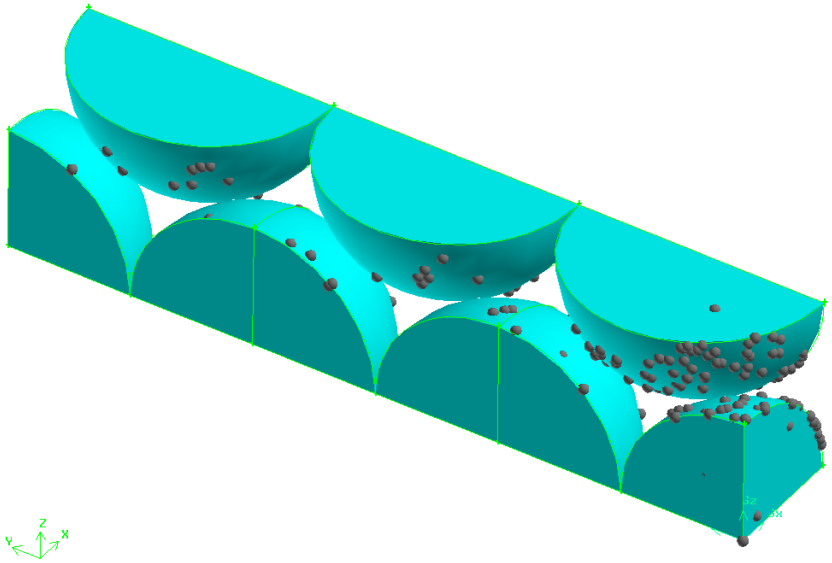

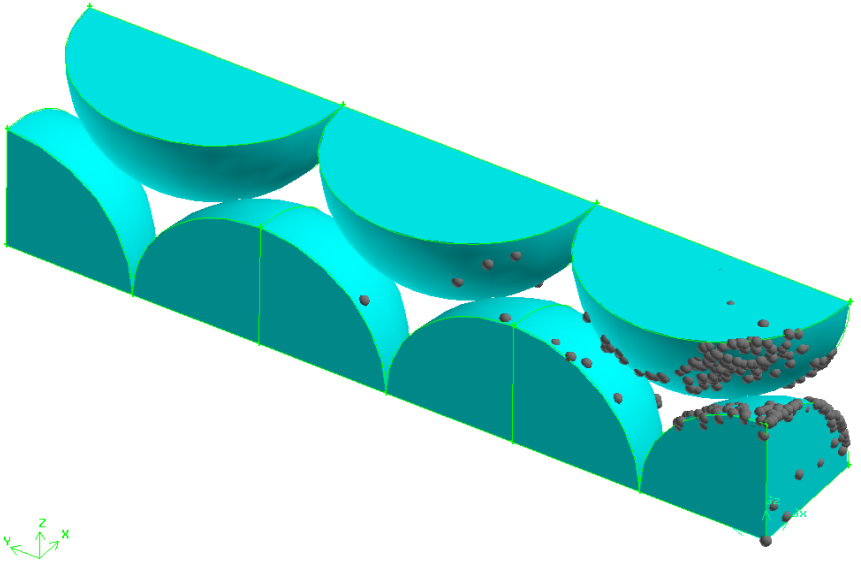

N=20

N=100

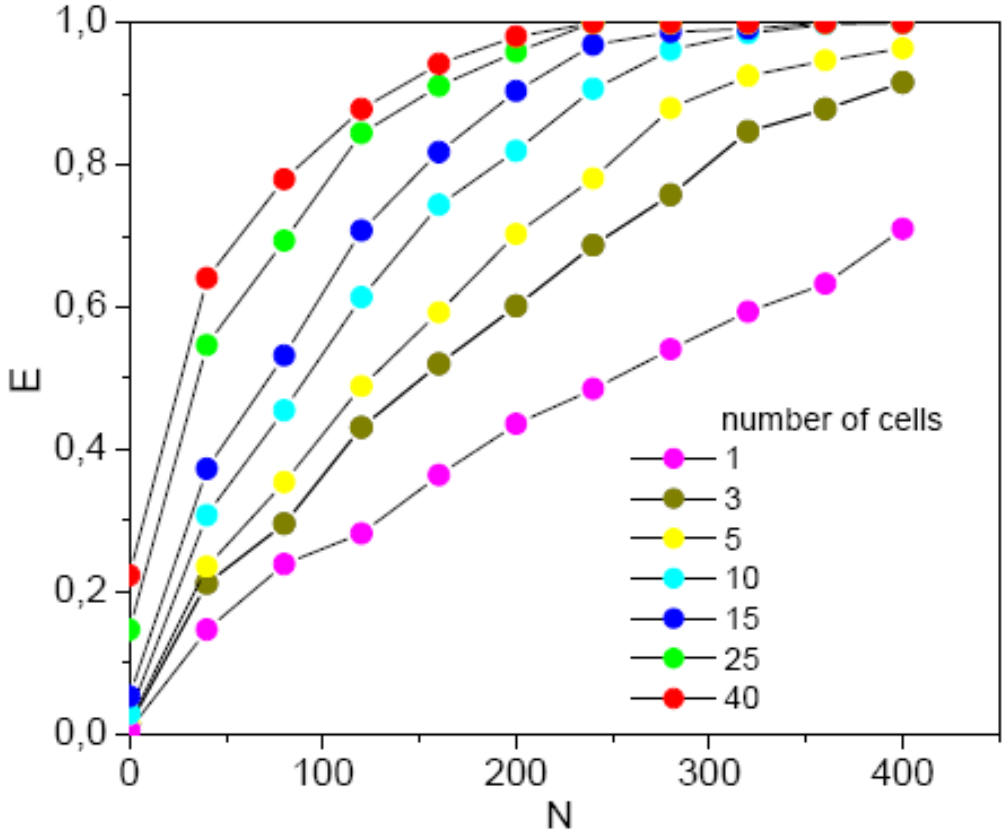

Fig.9.1 Depostion efficiency of charged particles for case 3 and d_p=0.6 μm at the various filter lengths (number of cells)

A.K. Gilfanov, W. Koch, S.K. Zaripov Mathematical modeling of di-ethyl-hexyl-sebacate nanoparticle formation in a free turbulent jet under high nucleation rate conditions. **Journal of Aerosol Science**. - 2016. - V.96. - P.124-139.

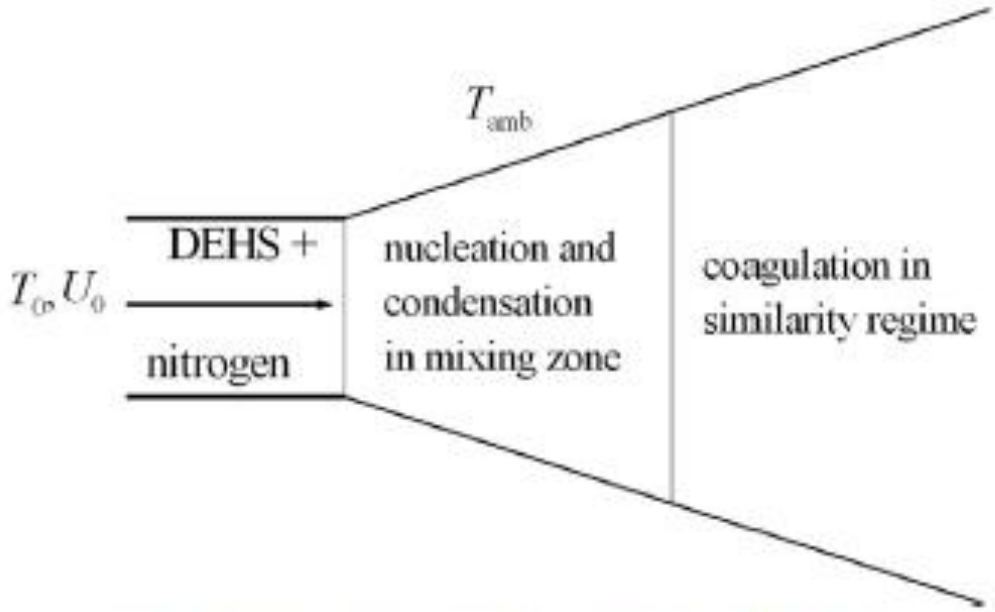

Fig. 1. Scheme of nanoparticle creation in a turbulent jet.

Collaboration
Brighton University - Kazan University
2016-2018

Joint project Royal Society (UK) RFBR (Russian Federation)

Modelling of aerosols/sprays for medical and automotive applications

Aerosol laboratory

- Head Prof. Shamil Zaripov, GAeF member

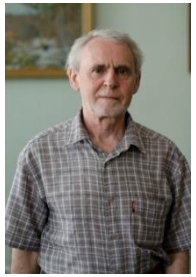

Founded in **1804**, Kazan University is the second oldest university in the Russian Federation, and now is an internationally acknowledged center of academic excellence.

Before 1878 Kazan University was the farthest Eastern university of the Russian Empire:
its academic district included the Volga Region, Kama Region, Ural Region, Siberia and Caucasus.

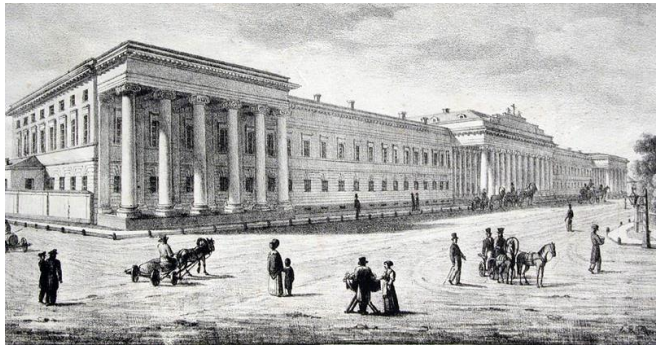

The main center of higher education for a vast region, KFU has over **47,000** students, who follow **310** major degree programs.

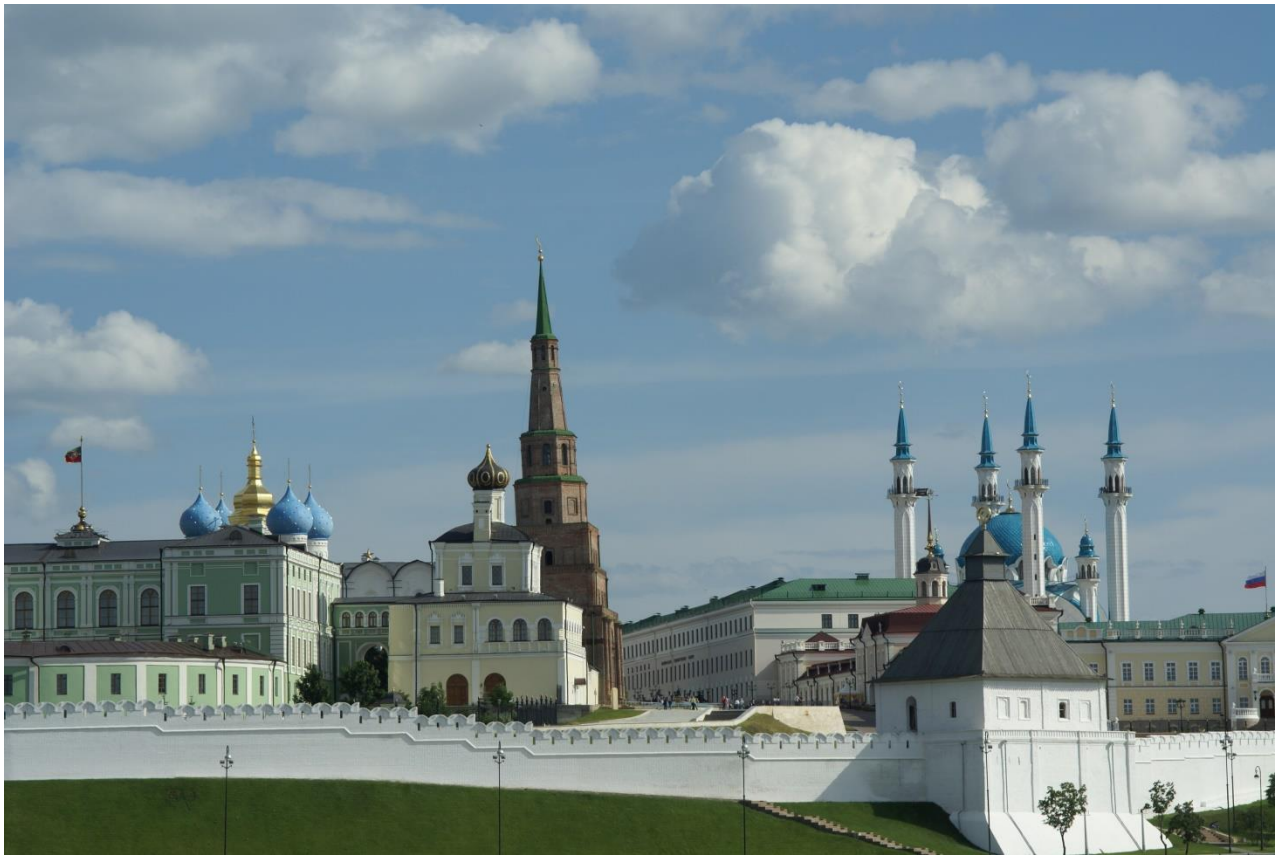

Thank you for attention